Passivity-Based Attitude Synchronization in $SE(3)$

Yuji Igarashi, Takeshi Hatanaka, *Member, IEEE*, Masayuki Fujita, *Member, IEEE*, and Mark W. Spong, *Fellow, IEEE*

***Abstract*—This paper addresses passivity-based motion coordination of rigid bodies in the Special Euclidean group $SE(3)$ under the assumption that the agents exchange information over strongly connected graphs. In this paper, we especially focus on one of the motion coordination problems on $SE(3)$ called attitude synchronization. We first develop a passivity-based distributed velocity input law to achieve attitude synchronization. Using the notion of algebraic connectivity, we then establish a connection between the speed of convergence and the structure of the interconnection graph. We also prove attitude synchronization in the leader-follower case and in the cases of communication delay and temporary communication failures. Finally, the performance of our developed control laws is demonstrated through both numerical simulation and experiments on a planar (2-D) test bed.**

***Index Terms*—Algebraic connectivity, attitude synchronization, cooperative control, motion coordination, passivity-based control.**

I. Introduction

MOTION coordination or cooperative control is an active area of current research [1], [2] with numerous practical applications such as sensor networks, robot networks, coordinated control of satellites and formation control of aircraft [3]–[7]. In addition, motion coordination is also motivated by scientific interest in cooperative behavior in nature such as flocking of birds and schooling of fishes [8]. The goal in cooperative control problems is to design a distributed control strategy using only local information so that the aggregate system attains specified behaviors, such as consensus [2], [9], flocking [12]–[16], synchronization [17], [18], or coordination [19].

Limitations on available information make the cooperative control problem challenging and require a theory and viewpoint quite different from conventional problems. Graph theory has been applied to the analysis of such problems where agents and their communication are represented by nodes and edges of a graph, respectively. In this approach, the graph Laplacian plays an especially important role in the analysis of convergence and connectivity of such distributed systems. The graph Laplacian has been utilized to prove consensus and flocking, analyze the connectivity, determine the convergence value and to construct team objective functions in several references [2], [7], [9], [23].

More recently, passivity and passivity-based control have proved useful for the problem of motion coordination of multi-agent systems [10], [11], [24]–[28], [32]. In [24], [25] passivity-based control laws are presented for output synchronization of networks of passive nonlinear systems. Output synchronization is proved by employing the sum of storage functions as a Lyapunov function candidate. As shown in these references, passivity-based control enables one to handle communication delays and switching topology within a unified (energy-based) framework. Likewise, in [26] and [27] passivity is used to study the problem of steering the differences between the outputs of agents to a prescribed compact set, and to address the formation control or path synchronization problem.

Motion coordination in non-Euclidean space is gaining increasing interest [10], [11], [19], [20], [22], [28]–[32], motivated by many practical systems such as underwater vehicles, satellites, and visual feedback systems. Reference [19] considers a model of identical planar particles whose phase variable evolves on the circle S^1, and designs steering control laws to stabilize the closed-loop system. They show global phase stabilization, circular formations and balancing in all-to-all communication which may be an unrealistic assumption in multi-agent systems. In contrast to [19], [29] and [30] attain global convergence in the presence of communication limitation. These control laws instead require information other than orientations of neighbors in order to use a consensus estimator. References [10], [11], [20], and [28] consider multiple rigid bodies with attitude dynamics represented by Euler-Lagrange equations, while the former part of [20] and [32] use a kinematic model. Note that [10], [11], [28], and [32] more or less use the notion of passivity. For the kinematic model, [32] presents a passivity-based velocity control law consisting only of the relative information, and [20] a control law which achieves global convergence by using a consensus estimator [21]. For the dynamical models, [10] and [20] present control laws achieving global convergence under the assumption that their own absolute angular velocities are available for control, where [10] uses an external input and [20] does not. Reference [20] also proposes a control input attaining local convergence based only on relative information. On the other hand, [28] proposes a passivity-based control law achieving global convergence, which uses only relative information but requires an external input.

In this paper, we address passivity-based attitude synchronization in $SE(3)$ based on some techniques developed in [24], [25], and [32]. Throughout this paper, we mean by attitude synchronization that all the rigid bodies' translational velocities are equal and orientations converge to a common value. We consider a group of rigid bodies in $SE(3)$ whose interconnection is

Manuscript received February 08, 2008; revised August 14, 2008. Manuscript received in final form January 25, 2009. First published June 10, 2009; current version published August 26, 2009. Recommended by Associate Editor M. Mesbahi. This work was supported in part by Grant-in-Aid for Scientific Research (C) No. 19560437 and by the U.S. National Science Foundation under Grant ECCS 07–25433.

Y. Igarashi is with the Advanced Technology R&D Center, Mitsubishi Electric Corporation, Amagasaki, Hyogo 661-8661, Japan (e-mail: igarashi@fl.ctrl.titech.ac.jp).

T. Hatanaka and M. Fujita are with the Department of Mechanical and Control Engineering, Tokyo Institute of Technology, Tokyo 152-8550, Japan (e-mail: hatanaka@ctrl.titech.ac.jp, fujita@ctrl.titech.ac.jp).

M. W. Spong is with the Erik Jonsson School of Engineering and Computer Science, University of Texas at Dallas, Dallas, TX 75080-3021 USA (e-mail: mspong@utdallas.edu).

Color versions of one or more of the figures in this paper are available online at http://ieeexplore.ieee.org.

Digital Object Identifier 10.1109/TCST.2009.2014357

represented by a strongly connected graph. First, we show that the kinematics of a rigid body in $SE(3)$ is passive. Then, we develop a passivity-based distributed velocity input law to achieve attitude synchronization under the condition that all the orientation matrices are positive definite. Namely, our proposed velocity control scheme does not achieve global convergence, but it is instead easy to implement, since it depends only on local relative information between its own reference frame and that of its neighbors.

We next introduce the notion of *algebraic connectivity* in order to establish a connection between the speed of convergence and the graph structure. The speed of convergence is a useful metric for the design of the information graph as well as for the analysis of the performance of cooperative control for a given network. Note that its counterpart in consensus has been extensively studied [2].

We also show attitude synchronization in the case of a leader-follower network and we address the practically important cases of time delays in communication, and temporary communication failures.

We finally show the performance of our control laws through numerical simulation and through experiments. Note that the experiments are performed on a planar (2-D) test bed.

The main contribution of this paper is to extend several standard results in consensus [2] (such as convergence, communication delays, leader following, connectivity analysis and switching topology) to a motion coordination problem in $SE(3)$, and to show that these problems can be handled within a unified energy-based framework. In addition, our work has the following technical advantages over other works on motion coordination in $SE(3)$ or $SO(3)$ [10], [11], [19], [20], [22], [28]–[30]: 1) only strong connectivity is assumed on the graph while other energy-based works require strongly connected balanced graphs or connected undirected graphs and 2) this paper clarifies a connection between the speed of convergence and the graph structure for attitude synchronization in $SE(3)$.

This paper is organized as follows. Section II formulates rigid-body motion in $SE(3)$ and the graph structure considered in this paper. In Section III, we first show that the rigid-body motion in $SE(3)$ is passive, and introduce the attitude synchronization problem. Then, an angular velocity control law is proposed based on passivity and achievement of attitude synchronization is proved. We also show if there are communication delays and/or a leader, attitude synchronization is still attained. Section IV analyzes the connectivity and possibility of communication losses. We demonstrate our results through numerical simulations and experiments in Section V and present conclusions in Section VI.

II. System Description

Throughout this paper, we consider the motion of a group of n rigid bodies in 3-D space (see Fig. 1). Let Σ_{w} be an inertial coordinate frame and Σ_i, $i \in \{1,\ldots,n\}$ a body-fixed coordinate frame whose origin is located at the center of mass of body i. Assume that all the coordinate frames are right-handed and Cartesian. We denote by $p_i \in \mathcal{R}^3$ the position of the rigid body $i \in \{1,\ldots,n\}$ in a fixed inertial coordinate frame Σ_{w}. We will use $e^{\hat{\xi}_i\theta_i} \in \mathcal{R}^{3\times 3}$ to represent the rotation matrix of a body-fixed frame Σ_i relative to an inertial coordinate frame Σ_{w}. Here, $\xi_i \in \mathcal{R}^3$, $\xi_i^T\xi_i = 1$ and $\theta_i \in \mathcal{R}$ specify the direction of rotation and the angle of rotation, respectively. The notation "$\wedge$" (wedge) is the skew-symmetric operator from $\mathcal{R}^3$ to the space of 3×3 skew-symmetric matrices, namely

$$\begin{bmatrix}\xi_1\\ \xi_2\\ \xi_3\end{bmatrix}^{\wedge} = \begin{bmatrix}0 & -\xi_3 & \xi_2\\ \xi_3 & 0 & -\xi_1\\ -\xi_2 & \xi_1 & 0\end{bmatrix}.$$

The notation "$\vee$" (vee) denotes the inverse operator to "$\wedge$". The transformation $e^{\hat{\xi}_i\theta_i}$ is orthogonal with unit determinant, i.e., an element of the Special Orthogonal group $SO(3)$. A configuration consists of the pair $(p_i, e^{\hat{\xi}_i\theta_i})$ and hence the configuration space of the rigid-body motion is the Special Euclidean group $SE(3)$, which is the product space of $\mathcal{R}^3$ with $SO(3)$. We use the 4×4 matrix

$$g_i = \begin{bmatrix}e^{\hat{\xi}_i\theta_i} & p_i\\ 0 & 1\end{bmatrix}, \quad i \in \{1,\ldots,n\}$$

as the homogeneous representation of $(p_i, e^{\hat{\xi}_i\theta_i}) \in SE(3)$.

Let us now introduce the velocity of each rigid body to represent the rigid-body motion of the frame Σ_i relative to Σ_{w}. Define the body velocity $V_i^b := (v_i, \omega_i)$ and

$$\hat{V}_i^b = \begin{bmatrix}\hat{\omega}_i & v_i\\ 0 & 0\end{bmatrix}, \quad i \in \{1,\ldots,n\}$$

where $v_i \in \mathcal{R}^3$ and $\omega_i \in \mathcal{R}^3$ are the linear and angular velocities of body i relative to Σ_i, respectively. Then, each rigid-body motion is represented by the kinematic model

$$\dot{g}_i = g_i\hat{V}_i^b, \quad i \in \{1,\ldots,n\}. \tag{1}$$

The main advantages to using the above homogeneous representation are global and geometric descriptions of rigid-body motion, which greatly simplify the analysis in the 3-D space. For more details on the rigid-body motion in $SE(3)$, refer to [33] and [34].

The interconnection of a network of rigid bodies is represented by a *weighted*, *directed*, and *strongly connected* graph $G = (\mathcal{V}, \mathcal{E}, \mathcal{W})$, where $\mathcal{V} := \{1,\ldots,n\}$, $\mathcal{E} \subset \mathcal{V}\times\mathcal{V}$ and $\mathcal{W}$ are the node set, the edge set and the positive weight set, respectively. The neighbors of body i are defined as [2]

$$\mathcal{N}_i := \{j \in \mathcal{V} \mid (j,i) \in \mathcal{E}\}.$$

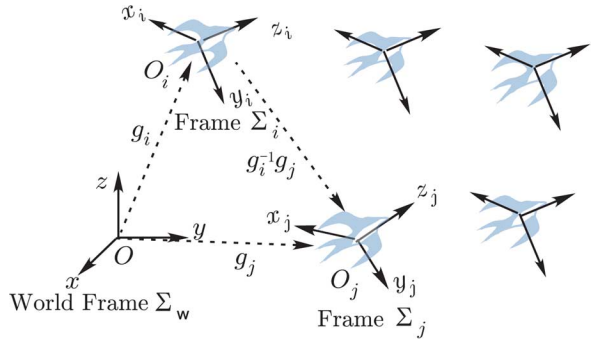

Fig. 1. Rigid-body motion in $SE(3)$.

Namely, agent i received information from agent j if $j \in \mathcal{N}_i$. The weights $w_{ij} > 0$ represent the reliability of each communication link. We moreover define the weighted graph Laplacian matrix

$$L_{\mathrm{w}} := [L_{\mathrm{w}ij}] = \begin{cases} \sum_{j \in \mathcal{N}_i} w_{ij}, & \text{if } j = i \\ -w_{ij}, & \text{if } j \in \mathcal{N}_i \\ 0, & \text{if } j \notin \mathcal{N}_i \end{cases}$$

which plays an important role in this paper.

III. Attitude Synchronization

In this section, we investigate the attitude synchronization problem in $SE(3)$. We first show that the kinematic model (1) is passive and we use this property to develop an output feedback law for attitude synchronization.

A. Passivity in $SE(3)$

We first define the *energy of rotation*

$$\phi\left(e^{\hat{\xi}_i\theta_i}\right) := \frac{1}{2}\mathrm{tr}(I_3 - e^{\hat{\xi}_i\theta_i}) \geq 0$$

where I_n is the $n \times n$ identity matrix. By the definition, $\phi(e^{\hat{\xi}_i\theta_i}) = 0$ if and only if $e^{\hat{\xi}_i\theta_i} = I_3$. Then, its derivative along the trajectories of (1) is given by

$$\dot{\phi}\left(e^{\hat{\xi}_i\theta_i}\right) = \left(\mathbf{sk}\left(e^{\hat{\xi}_i\theta_i}\right)^{\vee}\right)^T \omega_i \tag{2}$$

where

$$\mathbf{sk}\left(e^{\hat{\xi}_i\theta_i}\right) := \frac{1}{2}\left(e^{\hat{\xi}_i\theta_i} - e^{-\hat{\xi}_i\theta_i}\right).$$

(see, e.g., [34]). The term $\mathbf{sk}(e^{\hat{\xi}_i\theta_i})^{\vee}$ satisfies $\mathbf{sk}(e^{\hat{\xi}_i\theta_i})^{\vee} = \sin(\theta_i)\xi_i$, and hence $\mathbf{sk}(e^{\hat{\xi}_i\theta_i})^{\vee}$ is interpreted as an operator extracting the direction of rotation and the angle from $e^{\hat{\xi}_i\theta_i}$. Note that $\mathbf{sk}(e^{\hat{\xi}_i\theta_i})^{\vee}$ can also be viewed as the state vector with respect to the rotation as long as $|\theta_i| \leq \pi/2$ because of the fact that the rotational axis and the angle uniquely determine the rotation matrix if $|\theta_i| \leq \pi/2$. Thus, $\dot{\phi}(e^{\hat{\xi}_i\theta_i})$ is given by the inner product of the angular velocity and the state vector with respect to the rotation. Moreover, we define the total energy of translation and rotation

$$\begin{aligned} \psi(g_i) &:= \|(I_4 - g_i)J\|_F^2 \\ &= \frac{1}{2}\|p_i\|^2 + \phi(e^{\hat{\xi}_i\theta_i}) \\ J &:= \begin{bmatrix} \frac{1}{2}I_3 & 0 \\ 0 & \frac{1}{\sqrt{2}} \end{bmatrix} \end{aligned}$$

where $\|\cdot\|_F$ represents the Frobenius matrix norm ($\|A\|_F = \mathrm{tr}(A^TA)^{1/2}$) and $\|\cdot\|$ the Euclidean vector norm.

Lemma 1: The time derivative of $\psi(g_i)$ along the trajectories of (1) satisfies

$$\begin{aligned} \dot{\psi}(g_i) &= \left(V_i^b\right)^T \Pi_i \\ V_i^b &= \begin{bmatrix} v_i \\ \omega_i \end{bmatrix} \\ \Pi_i &:= \begin{bmatrix} e^{-\hat{\xi}_i\theta_i}p_i \\ \mathbf{sk}(e^{\hat{\xi}_i\theta_i})^{\vee} \end{bmatrix}. \end{aligned} \tag{3}$$

Proof: Immediate from [35, pp. 42, Lemma 1]. ■

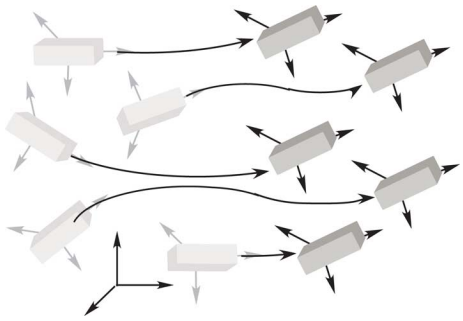

Fig. 2. Attitude synchronization in $SE(3)$.

If we now consider the velocity V_i^b as an input and the vector form of the rigid-body motion Π_i as an output, Lemma 1 says that the rigid-body motion in $SE(3)$ (1) is passive from the input V_i^b to the output Π_i in the sense defined in [36], since integrating (3) from 0 to T yields

$$\int_0^T (V_i^b)^T \Pi_i dt = \psi(g_i(T)) - \psi(g_i(0)) \geq -\psi(g_i(0)). \tag{4}$$

B. Attitude Synchronization in $SE(3)$

The goal of this section is to design the velocity input V_i^b so that the group of rigid bodies achieves attitude synchronization in the sense of the following definition.

Definition 1: A group of rigid bodies is said to achieve attitude synchronization, if $v_i = v_j \,\forall\, i, j \in \{1, \ldots, n\}$ and

$$\lim_{t\to\infty} \phi(e^{-\hat{\xi}_i\theta_i}e^{\hat{\xi}_j\theta_j}) = 0 \,\forall\, i, \quad j \in \{1, \ldots, n\}. \tag{5}$$

Equation (5) implies that the orientations of all the rigid bodies asymptotically converge to a common value (see Fig. 2).

According to the above definition of attitude synchronization, in the remainder of this section we fix

$$v_i = v_j \,\forall\, i, j \in \{1, \ldots, n\} \tag{6}$$

in the input terms V_i^b, and present an angular velocity control law that achieves attitude synchronization. It is clear from Lemma 1 that the kinematic model (1) is also passive from ω_i to $\mathbf{sk}(e^{\hat{\xi}_i\theta_i})^{\vee}$ with the storage function $\phi(e^{\hat{\xi}_i\theta_i})$.

We propose the angular velocity control law

$$\omega_i = k_i \sum_{j \in \mathcal{N}_i} w_{ij} \mathbf{sk}\left(e^{-\hat{\xi}_i\theta_i}e^{\hat{\xi}_j\theta_j}\right)^{\vee}, \quad i \in \{1, \ldots, n\} \tag{7}$$

where $k_i > 0$ are feedback gains. This control law is distributed, i.e., is composed only of the rigid body's own information and that of its neighbors. It should, in addition, be noted that $e^{-\hat{\xi}_i\theta_i}e^{\hat{\xi}_j\theta_j}$ is the relative orientation of rigid body j from the frame Σ_i and hence the angular velocity law (7) does not require $e^{\hat{\xi}_j\theta_j}$ itself.

As a consequence of Lemma 1, we have the following theorem. Throughout this paper, we refer to a real matrix Q, which is not necessarily symmetric, as a positive definite (positive semi-definite) matrix if and only if $x^TQx > 0$ ($x^TQx \geq 0$) for all nonzero vector x.

Theorem 1: Consider the n rigid bodies represented by (1). Under the assumptions that all rigid body orientation matrices are positive definite and the interconnection graph is fixed and strongly connected, the angular velocity control input (7) achieves attitude synchronization in the sense of (5).

Proof: See Appendix A. ■

Remarks:

1) In the proof of Theorem 1, a potential function U_{A} is defined as a weighted sum of the energy functions of rotation $\phi(e^{\hat{\xi}_i\theta_i})$ and used as a Lyapunov function candidate. This choice is quite natural from the viewpoint that the kinematic model (4) is passive. In addition, this potential function enables us to remove the balanced graph assumption of earlier approaches, e.g., [24], [25], and thus prove attitude synchronization for a wider class of information graphs, namely, strongly connected graphs.
2) If the rotation matrix $e^{\hat{\xi}_i\theta_i}$ and linear velocity v_i are given by

$$e^{\hat{\xi}_i\theta_i} = \begin{bmatrix} \cos\theta_i & -\sin\theta_i & 0 \\ \sin\theta_i & \cos\theta_i & 0 \\ 0 & 0 & 1 \end{bmatrix}$$
$$v_i = \begin{bmatrix} 1 \\ 0 \\ 0 \end{bmatrix} \quad \forall\, i \in \{1, \ldots, n\} \tag{8}$$

the kinematics model (1) is equivalent to the 2-D model considered in [14]. If the rotation matrix and linear velocity are represented by Z-Y-Z Euler angles and $\begin{bmatrix} 0 & 0 & 1 \end{bmatrix}^T$, respectively, then (1) is equivalent to the 3-D case in the above reference. It should be noted that [14] takes into account a nonholonomic constraint, whereas this paper does not since we are interested in the full 3-D motion.
3) The inequality $|\theta_i| < \pi/2$ is necessary and sufficient to satisfy the assumption that all rigid bodies orientation matrices are positive definite. Note that the satisfaction of this inequality at the initial time implies that it holds for all time $t \geq 0$ as shown in the following Lemma.

Lemma 2: Consider the n rigid bodies represented by (1). Suppose that the angular velocity (7) is the input to each rigid body. If all rigid body orientation matrices are positive definite at the initial time, then they remain positive definite for all time $t \geq 0$.

Proof: See Appendix B. ■

A similar assumption appears in [14], [17], [18], and [37]. Note that there are several works investigating global convergence. For example, the [19] assures it under the assumption of all-to-all communication, which may be a strong assumption on graphs. On the other hand, [20], [29], and [30] investigate global convergence in the presence of communicative limitation. However, these control laws require information other than the orientations of neighbors due to the use of a consensus estimator. In addition, global convergence is also achieved in [10] under the assumption that all the rigid bodies know their own attitude with respect to the inertial frame. In contrast to these works, due to the assumption $|\theta_i(0)| < \pi/2$, we may have to initially align the rigid bodies by determining their orientation axes in order to satisfy $|\theta_i(0)| < \pi/2\ \forall\, i$. However, our result is instead applicable to the situation where only the relative orientation is available for control and communication is more limited as long as the graph is strongly connected.

4) Reference [9] presents a consensus algorithm under the assumption that the information graph has a directed spanning tree, which is a weaker condition than the strong connectivity. However, in $SE(3)$, it is difficult to adopt the approach of [9], which is based on eigenvalue analysis. Though balanced or undirected graphs are assumed in most previous research works adopting approaches other than eigenvalue analysis [2], [14], [16], [20], [28], we assume neither of them. Meanwhile, in [38] and [39] a state-dependent weighted graph is investigated to maintain connectedness while the weights are time-invariant and independent of the state in [2], [16], and this paper. Note that these are completely different assumptions. Indeed the former assumes that the weights are symmetric, i.e., $w_{ij} = w_{ji}$, whereas the latter does not require it.
5) Though the problems under consideration are quite different from ours, passivity-based motion coordination is also investigated in [26] and [27], which suggests that passivity is a useful tool in motion coordination.
6) The final orientation value depends on the initial configuration of the system and on the graph. We are not aware of any research that tries to find the convergence value in $SO(3)$, while a convergence value is clarified in the case of the Euclidean space in [2] and [23].
7) The velocity input (7) achieves not only (5) but also

$$\lim_{t\to\infty} \|\dot{p}_i - \dot{p}_j\| = 0 \quad \forall\, i, j \in \{1, \ldots, n\} \tag{9}$$

for the following reason. Equation (1) yields

$$\begin{aligned} \hat{V}_i^b &= g_i^{-1}\dot{g}_i \\ \begin{bmatrix} \hat{\omega}_i & v_i \\ 0 & 0 \end{bmatrix} &= \begin{bmatrix} e^{-\hat{\xi}_i\theta_i} & -e^{-\hat{\xi}_i\theta_i}p_i \\ 0 & 1 \end{bmatrix} \begin{bmatrix} e^{\hat{\xi}_i\theta_i}\hat{\omega}_i & \dot{p}_i \\ 0 & 0 \end{bmatrix} \\ &= \begin{bmatrix} \hat{\omega}_i & e^{-\hat{\xi}_i\theta_i}\dot{p}_i \\ 0 & 0 \end{bmatrix}. \end{aligned} \tag{10}$$

Focusing on the (1,2)-element of (10), we obtain $\dot{p}_i = e^{\hat{\xi}_i\theta_i}v_i$. It follows from (5) and (6) that the present velocity input also achieves (9). The property (9) is called flocking in [13], [15], and [16]. We add $v_i = v_j\ \forall i, j$ to the definition of attitude coordination in order to assure the (9). Indeed, without $v_i = v_j\ \forall i, j$, all the rigid bodies go in different directions while their attitudes converge to the same.

C. Communication Delays

In this section, we consider attitude synchronization in the presence of communication delays. We assume that the delay is time invariant and finite, which is the same situation as [24] and [25].

In this case, attitude synchronization is redefined as

$$\lim_{t\to\infty} \phi\left(e^{-\hat{\xi}_i(t-T_{ij})\theta_i(t-T_{ij})}e^{\hat{\xi}_j(t)\theta_j(t)}\right) = 0 \quad \forall\, i, j \in \{1, \ldots, n\},\ i \neq j \tag{11}$$

where $T_{ij} \geq 0$ is the delay in the communication from agent i to agent j. Accordingly, we modify the input (7) as

$$\omega_i = k_i \sum_{j \in \mathcal{N}_i} w_{ij} \mathbf{sk}(e^{-\hat{\xi}_i(t)\theta_i(t)} e^{\hat{\xi}_j(t-T_{ji})\theta_j(t-T_{ji})})^\vee, \quad k_i > 0, \quad i \in \{1, \ldots, n\} \tag{12}$$

based on [24] and [25]. Then, we have the following corollary.

Corollary 1: Consider the n rigid bodies represented by (1). Then, under the assumption that all rigid body orientation matrices are positive definite, and the interconnection graph is fixed and strongly connected, the velocity input (12) achieves attitude synchronization in the sense of (11).

Proof: This corollary is proved in the same way as Theorem 1 by using the potential function

$$U_{\text{delay}} := \sum_{i=1}^{n} \frac{\gamma_i}{k_i} \phi(e^{\hat{\xi}_i(t)\theta_i(t)}) + \sum_{i=1}^{n} \sum_{j \in \mathcal{N}_i} \gamma_i w_{ij} \int_{t-T_{ji}}^{t} \phi(e^{\hat{\xi}_i(\tau)\theta_i(\tau)}) d\tau.$$

■

Remark that the control input (12) does not consist of relative information with respect to neighbors and all the neighbors have to communicate to agent i their own attitude matrices with respect to the inertial frame, which is different than the other part of this paper. This implies that all the agents should share the same inertial frame in contrast to the delay free case.

D. Leader Following

We consider here the case that one rigid body, labeled 0, acts as a leader as in [12] and [14]. Suppose that rigid body 0 moves with a constant velocity and orientation. Other agents may or may not have the leader as a neighbor. In this case, attitude synchronization is defined by

$$\lim_{t \to \infty} \phi(e^{-\hat{\xi}_i \theta_i} e^{\hat{\xi}_0 \theta_0}) = 0 \quad \forall\, i \in \{1, \ldots, n\} \tag{13}$$

which means that the orientations of all agents converge to the orientation of the leader. In this case, we modify the angular velocity input (7) as

$$\omega_i = k_i \left(\sum_{j \in \mathcal{N}_i} w_{ij} \mathbf{sk}(e^{-\hat{\xi}_i \theta_i} e^{\hat{\xi}_j \theta_j})^\vee + c_i w_{i0} \mathbf{sk}(e^{-\hat{\xi}_i \theta_i} e^{\hat{\xi}_0 \theta_0})^\vee \right), \quad k_i, w_{i0} > 0, \quad i \in \{1, \ldots, n\} \tag{14}$$

where $c_i = 1$ if rigid body i and the leader are neighbors and $c_i = 0$ otherwise. With this control input we have the following corollary.

Corollary 2: Consider the n rigid bodies represented by (1) and the leader moving with a constant velocity and orientation. The angular velocity (14) achieves attitude synchronization in the sense of (13) if it follows that:

1) the relative orientation matrices between the leader and the agents are positive definite;
2) the interconnection graph excluding the leader is fixed and strongly connected;
3) there exists at least one i satisfying $c_i = 1$.

Proof: This corollary can be easily proved by using the potential function

$$U_{\text{leader}} := \sum_{i=1}^{n} \frac{\gamma_i}{k_i} \phi(e^{-\hat{\xi}_i \theta_i} e^{\hat{\xi}_0 \theta_0}).$$

■

In Section III-C, we stated that the final orientation value is determined by the initial configuration (Remark 6). On the other hand, in the leader-follower case, the orientations of all agents converge to the leader's orientation. Of course, we can converge all agents' orientations to a desired one if it is chosen as the leader's orientation.

IV. Connectivity Analysis

A. Algebraic Connectivity

The purpose of this section is to analyze the relationship between the graph structure and the speed of convergence of the network to its final configuration. We first introduce an index U_{exp} evaluating the speed of convergence. In order to measure the speed, U_{exp} should satisfy the following two conditions:

1) attitude synchronization is achieved if and only if $\lim_{t \to \infty} U_{\text{exp}} = 0$ holds;
2) $U_{\text{exp}}(0)$ is independent of the graph.

Note that the function $U_{\text{A}} = \sum_{i=1}^{n} \gamma_i / k_i \ \phi(e^{\hat{\xi}_i \theta_i}) = \sum_{i=1}^{n} \gamma_i / 2k_i \ \text{tr}\left(I - e^{\hat{\xi}_i \theta_i}\right)$ defined in Appendix A does not satisfy condition 1) and it is necessary to consider a different function. Olfati-Saber *et al.* [2] employs a function evaluating the error between the position of each agent and the convergence value. However, this type of function cannot be used directly since the convergence value is unknown in this paper. Alternatively, functions of the orientation errors between rigid bodies also satisfy condition 1), and such a function can be easily constructed by using the graph Laplacian L_{w}. However, the use of L_{w} is prohibited due to condition 2). For the above reasons, we define the function

$$U_{\text{exp}}(t) := \text{tr}\left((e^{\hat{\xi}(t)\theta(t)})^T (M \otimes I_3) e^{\hat{\xi}(t)\theta(t)} \right) = 2 \sum_{i=1}^{n} \sum_{j=1}^{n} \phi(e^{-\hat{\xi}_i \theta_i} e^{\hat{\xi}_j \theta_j}) \geq 0$$

to evaluate the speed of convergence, where M denotes the graph Laplacian of the nonweighted complete graph (i.e., $w_{ij} = 1 \ \forall\, i, j$), namely

$$M := n I_n - \mathbf{1}_n \mathbf{1}_n^T$$

where $\mathbf{1}_n := [1, \ldots, 1]^T \in \mathcal{R}^n$ and $e^{\hat{\xi}(t)\theta(t)} := [e^{-\hat{\xi}_1(t)\theta_1(t)}, \ldots, e^{-\hat{\xi}_n(t)\theta_n(t)}]^T$. This function evaluates the relative orientation for all rigid bodies regardless of the actual connectivity, and satisfies both of the above conditions. Notice that the potential function U_{A}, in the previous section is defined by the individual agent's energy functions $\phi(e^{\hat{\xi}_i \theta_i})$, rather that the energy of the relative orientations.

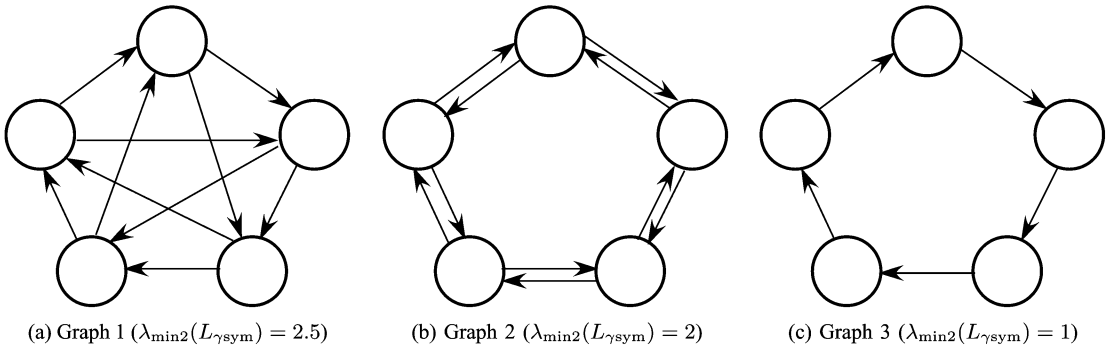

(a) Graph 1 ($\lambda_{\min 2}(L_{\gamma \mathrm{sym}}) = 2.5$) (b) Graph 2 ($\lambda_{\min 2}(L_{\gamma \mathrm{sym}}) = 2$) (c) Graph 3 ($\lambda_{\min 2}(L_{\gamma \mathrm{sym}}) = 1$)

Fig. 3. Second smallest eigenvalues of $L_{\gamma \mathrm{sym}}$ for various information graphs.

Before stating the main result of this section, we introduce the following notation. Let $L_{\mathrm{sym}} := 1/2(L + L^T)$ denote the symmetric part of a matrix L. The notation $\mathrm{diag}(\gamma_1, \ldots, \gamma_n)$ represents the diagonal matrix with diagonal elements $\gamma_1, \ldots, \gamma_n$ and L_γ denotes $L_\gamma := \mathrm{diag}(\gamma_1, \ldots, \gamma_n) L_{\mathrm{w}}$, where $\gamma^T L_{\mathrm{w}} = 0$, $\gamma := [\gamma_1, \ldots, \gamma_n]^T$. Let $\lambda_{\min}(L)$ and $\lambda_{\min 2}(L)$ be the smallest eigenvalue and the second smallest eigenvalue, respectively, of any real symmetric square matrix L. We can now state the following.

Theorem 2: Consider the n rigid bodies represented by (1). Then, under the assumption that the relative orientations, $e^{-\hat{\xi}_i \theta_i} e^{\hat{\xi}_j \theta_j}$ $\forall i, j$, are positive definite, there exist positive real numbers a_e and b_e such that

$$U_{\exp}(t) \leq a_e U_{\exp}(0) e^{-\lambda_{\min 2}(L_{\gamma \mathrm{sym}}) b_e t}. \tag{15}$$

Proof: Appendix C ■

Because of the independence of $U_{\exp}(0)$ on the graph structure, Theorem 2 implies that the larger the value of $\lambda_{\min 2}(L_{\gamma \mathrm{sym}})$ for a given graph, the faster the right-hand side of (15) converges to 0. In general, $\lambda_{\min 2}(L_{\gamma \mathrm{sym}})$ is called *algebraic connectivity* of a graph, and it is well-known in consensus [2] that it is a measure of the speed of convergence.

Generally speaking, the graph with many distributed edges has a large algebraic connectivity. In order to illustrate it, we prepare three graphs in Fig. 3, where all the edges have weights 1. Graph 1 has a larger $\lambda_{\min 2}(L_{\gamma \mathrm{sym}})$ than Graph 2, which illustrates that the algebraic connectivity of a graph with distributed edges is large, and Graphs 2 also has a larger $\lambda_{\min 2}(L_{\gamma \mathrm{sym}})$ than Graph 3, which indicates the fact that the algebraic connectivity of a graph with many edges is large. These facts imply that the algebraic connectivity and hence the speed of convergence depend not only on the number of edges but also on their distribution. Reference [40] investigates the problem of choosing the weights of an undirected graph so as to maximize or minimize some function of the eigenvalues of the associated graph Laplacian, and [41] and [42] propose methods to maximize the second smallest eigenvalue of the graph Laplacian of the state dependent graph.

Theorem 2 also gives another important insight into convergence analysis. In the inequality (15), the error of orientations between rigid bodies exponentially converges to 0, though Theorem 1 only shows asymptotic convergence. Notice that Theorem 2 assumes the positive definiteness of the *relative* orientations, while Theorem 1 that of the *individual* orientations. Theorem 2 at least guarantees a type of local exponential convergence even with the initial conditions of Theorem 1 since, eventually, the relative orientations will converge to value less than $\pi/2$, at which time the remaining convergence will be exponential. An assumption similar to Theorem 2 is made in [17], where exponential synchronization is proved.

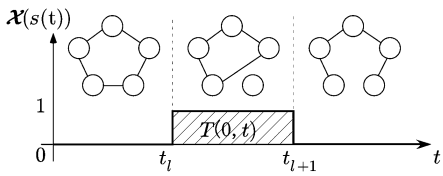

Fig. 4. Brief connectivity loss.

B. Brief Connectivity Loss

In this section, we investigate the situation where the information graph changes over time. Although other interpretations may be possible, we suppose that the disconnection represents communication failures. To study the effect of communication failures we utilize the concept of brief instability developed in [43]. This concept will be instrumental in capturing the fraction of the time that the graph may remain disconnected (see Fig. 4).

Let $\mathcal{G}$ be a certain set of possible graphs with n nodes and let $s(t) : [0, \infty] \rightarrow \mathcal{G}$ be the piecewise constant switching signal with consecutive switching times separated by a dwell time, $\tau_D > 0$. Namely, any two consecutive switching times t_l and t_{l+1}, $l \geq \{0, 1, 2, \ldots\}$ satisfy $t_{l+1} - t_l \geq \tau_D$, $l \geq 0$. The signal $s(t)$ belongs to either the following subsets of $\mathcal{G}$:

1) $\mathcal{G}_{\mathrm{c}} \subseteq \mathcal{G}$: a subset composed of strongly connected graphs;
2) $\mathcal{G}_{\mathrm{dc}} \subseteq \mathcal{G}$: a subset composed of not strongly connected graphs.

It is obvious from the definitions that $\mathcal{G} = \mathcal{G}_{\mathrm{c}} \cup \mathcal{G}_{\mathrm{dc}}$ holds true. Let us now introduce the connectivity loss time $T(\tau, t)$, which is the length of the time when the graph belongs to $\mathcal{G}_{\mathrm{dc}}$ over any time interval $[\tau, t]$. The function $T(\tau, t)$ is clearly given by

$$T(\tau, t) = \int_\tau^t \mathcal{X}(s(r)) dr$$

$$\mathcal{X}(s(t)) := \begin{cases} 0, & s(t) \in \mathcal{G}_{\mathrm{c}} \\ 1, & s(t) \in \mathcal{G}_{\mathrm{dc}}. \end{cases}$$

Brief connectivity losses [43] means

$$T(\tau, t) \leq \alpha(t - \tau) + T_0 \quad \forall\, t \geq \tau \geq 0 \tag{16}$$

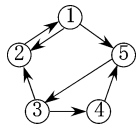

Fig. 5. Graph Topology (Simulation 1).

holds for some $T_0 \geq 0$ and $0 \leq \alpha < 1$. The scalar value α is called the asymptotic connectivity loss rate, and T_0 is called the connectivity loss bound.

Theorem 3: Consider the n rigid bodies represented by (1). Assume that the relative orientations, $e^{-\hat{\xi}_i\theta_i}e^{\hat{\xi}_j\theta_j}\ \forall i,j$, are positive definite. Then, if the inequalities (16) holds, there exists a lower bound of τ_D such that the angular velocity (7) achieves attitude synchronization in the sense of (5).

Proof: See Appendix D. ■

Roughly speaking, the inequality (16) means that the fraction of the connectivity loss time is small, and the existence of a lower bound of τ_D assures that the graph does not switch frequently.

In previous works, various approaches are adopted to deal with switching topology, for example, in [9], [12], [13], [16], [24], [25], and [44] where the concepts of joint connectedness, nonsmooth analysis, dwell time and uniform connectedness are all employed. Note that some works [12], [13], [24], [25], [44] among them handle a wider class of switching graphs than this paper, though they consider motion coordination not in $SE(3)$ but in the $\mathcal{R}^n$.

V. Numerical Simulations and Experiments

In this section, we demonstrate the effectiveness of our results by numerical simulation and experiments carried out on a mobile robot test bed. Specifically, Theorem 1 (attitude synchronization) is demonstrated through both simulations and experiments, Theorem 3 (switching topology) is demonstrated through simulations, and Theorem 2 (speed of convergence) is demonstrated through experiments.

A. Numerical Simulations

1) Simulation 1 (Attitude Synchronization): In this simulation we show numerically that the angular velocity (7) with $k_i = 1, i \in \{1,\dots,5\}$ attains attitude synchronization. In our simulations the group consists of five rigid bodies with the kinematics described by (1).

We first demonstrate the results in Section IV assuming the information graph structure with $w_{ij} = 1, (j,i) \in \mathcal{E}$ depicted in Fig. 5. Note that this graph is strongly connected but is not balanced. We run the simulation under the following initial conditions.

$$\begin{aligned} p_1(0) &= [1 \quad 0 \quad 3]^T \\ \xi_1(0)\theta_1(0) &= [-0.21 \quad -0.50 \quad 0.77]^T \\ p_2(0) &= [2 \quad -1 \quad 2]^T \\ \xi_2(0)\theta_2(0) &= [0.52 \quad -0.76 \quad 0.52]^T \\ p_3(0) &= [3 \quad 1 \quad 2]^T \\ \xi_3(0)\theta_3(0) &= [-0.21 \quad 0.77 \quad -0.50]^T \\ p_4(0) &= [-1 \quad -2 \quad 0]^T \\ \xi_4(0)\theta_4(0) &= [-0.14 \quad 0.51 \quad -0.51]^T \\ p_5(0) &= [0 \quad 0 \quad 0]^T \\ \xi_5(0)\theta_5(0) &= [0 \quad 1.05 \quad 0]^T. \end{aligned}$$

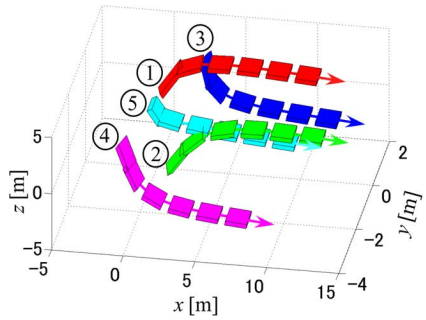

Fig. 6. Trajectories of the rigid bodies (Simulation 1).

We remark that the orientation matrices are positive definite at the initial time. Figs. 6 and 7 show the trajectories of the rigid bodies and rotation vectors $\xi_i\theta_i$. In Fig. 6, the encircled number is associated with the corresponding one in Fig. 5. We see from Fig. 6 that the rigid bodies smoothly adjust their orientation and move in the same direction. In Fig. 7, the rotation vectors $\xi_i\theta_i$ asymptotically converge to a common vector. From these figures, we can confirm that attitude synchronization is achieved by the angular velocity input (7).

2) Simulation 2 (Switching Topology): We next investigate the switching topology and confirm that attitude synchronization is still achieved. The initial states are changed as below since the relative orientation matrices should be positive definite

$$\begin{aligned} p_1(0) &= [1 \quad 0 \quad 3]^T \\ \xi_1(0)\theta_1(0) &= [-0.07 \quad -0.24 \quad 0.52]^T \\ p_2(0) &= [2 \quad -1 \quad 2]^T \\ \xi_2(0)\theta_2(0) &= [0.44 \quad -0.38 \quad 0.44]^T \\ p_3(0) &= [3 \quad 1 \quad 2]^T \\ \xi_3(0)\theta_3(0) &= [-0.13 \quad 0.51 \quad -0.51]^T \\ p_4(0) &= [-1 \quad -2 \quad 0]^T \\ \xi_4(0)\theta_4(0) &= [-0.14 \quad 0.51 \quad -0.51]^T \\ p_5(0) &= [0 \quad 0 \quad 0]^T \\ \xi_5(0)\theta_5(0) &= [0 \quad 1.05 \quad 0]^T. \end{aligned}$$

In this simulation, two types of graphs are repeated periodically every 2[s] (see Fig. 8), where one belongs to $\mathcal{G}_c$ and another $\mathcal{G}_{dc}$. Suppose that the graph is strongly connected at the initial time. Since these graphs are balanced, the weighted graph Laplacian L_w satisfies $\mathbf{1}^T L_w = 0$. Thus, $\gamma = \mathbf{1}$ and $L_\gamma = L_w$. Due to the change of the graph, the connectivity loss time $T(0,t)$ satisfies $T(0,t) \leq 1/2t$, namely $\alpha = 1/2, T_0 = 0$. In this simulation, the lower bound of τ_D should be greater than 0 in order to achieve attitude synchronization. Similarly to the previous simulation, Fig. 9 shows the trajectories of the position and orientation of each rigid body, and Fig. 10 the rotation vector

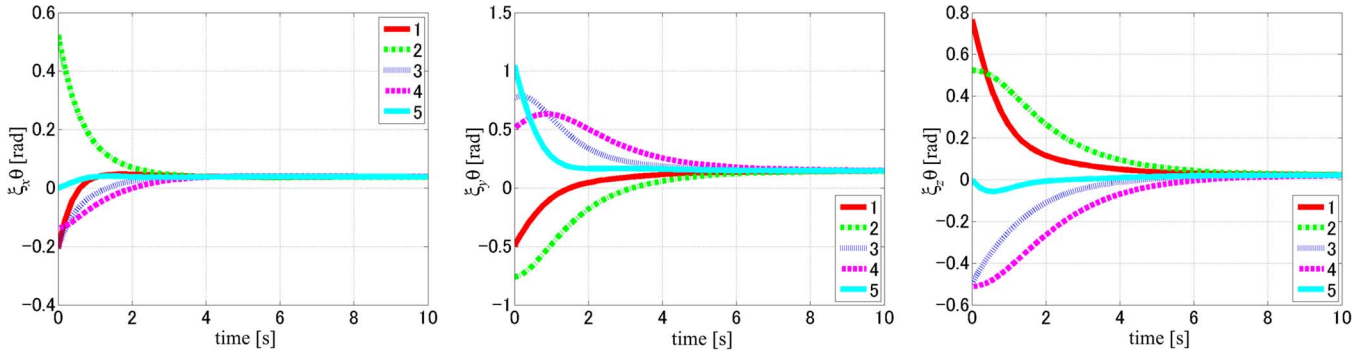

Fig. 7. Time responses of rotation vector $\xi_i\theta_i$ (Simulation 1).

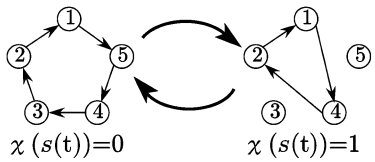

Fig. 8. Graph topology (Simulation 2).

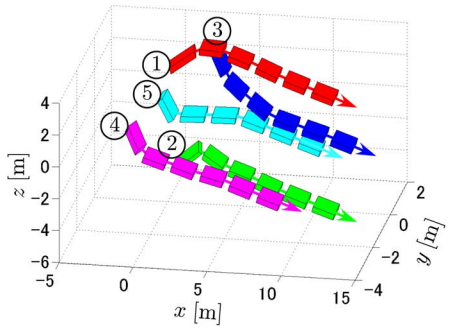

Fig. 9. Trajectories of the rigid bodies (Simulation 2).

$\xi_i\theta_i$. We see from Fig. 9 that all the rigid bodies eventually converge to a common orientation and move toward the same direction. Fig. 10 illustrates that $\xi_i\theta_i$ asymptotically converge to a common vector. These results suggest that attitude synchronization is achieved even in the switching topology case.

B. Experiments

In this section we present the experimental results on a planar (2-D) test bed. If the rotation matrix $e^{\hat{\xi}_i\theta_i}$ and linear velocity v_i are set as

$$e^{\hat{\xi}_i\theta_i} = \begin{bmatrix} \cos\theta_i & -\sin\theta_i & 0 \\ \sin\theta_i & \cos\theta_i & 0 \\ 0 & 0 & 1 \end{bmatrix}$$

$$v_i = \begin{bmatrix} 1 \\ 0 \\ 0 \end{bmatrix}, \quad i \in \{1, \ldots, 4\}$$

then the kinematics model (1) is equivalent to the 2-D case. Fig. 11 illustrates the experimental environment including the vehicles, camera, PC, and CF transmitters. The four vehicles (Fig. 12) are controlled by a digital signal processor (DSP) from dSPACE Inc., which utilizes a power PC running at 2.8 GHz. Control programs are written in MATLAB and SIMULINK, and implemented on the DSP using the real-time workshop and dSPACE Software such as ControlDesk, RealTime Interface, and so on. The DSP energizes the RF transmitters, which send commands to the vehicles. An MTV-7310 camera is mounted above the vehicles and has a resolution of 470×570.

The video signals are available in real time via a frame grabber board PicPort-Stereo-HrD and image processing software HALCON. The sampling period of the controller and the frame rate provided by the camera are 0.001[s] and 30[fps], respectively. The positions and orientations of the rigid bodies are calculated from the image data. Note that the experimental test bed is currently not distributed and the present law is implemented in a centralized way. In order to implement kinematic control on the vehicle network, we first designed a local PI controller *a priori* to track reference signals and then input the kinematic control laws as velocity reference signals (see Fig. 13). The total control system is depicted in Fig. 14, which illustrates only two rigid bodies for simplicity.

Fig. 15 shows a graph from this experiment. The control gain $k_i = 0.125, \forall\, i$ is empirically selected. Let the weights of the graph be $w_{ij} = 1, (j, i) \in \mathcal{E}$. The experiment is carried out with the initial conditions

$$\begin{aligned} p_1(0) &= [0.14 \quad 0.39]^T \text{ m} \quad \theta_1(0) = -67.1^\circ \\ p_2(0) &= [0.12 \quad 0.61]^T \text{ m} \quad \theta_2(0) = -43.0^\circ \\ p_3(0) &= [0.97 \quad 0.87]^T \text{ m} \quad \theta_3(0) = 80.6^\circ \\ p_4(0) &= [0.31 \quad 0.85]^T \text{ m} \quad \theta_4(0) = 0.18^\circ. \end{aligned} \tag{17}$$

The experimental results are shown in Figs. 16 and 17, which illustrate the orientation and position of the vehicles, respectively. In Fig. 9, the circles denote the initial positions of the vehicles. We can see from Fig. 16 that the orientations of the vehicles asymptotically converge to a common value and from Fig. 9 that vehicles eventually move in the same direction.

We next demonstrate the speed of convergence of attitude synchronization for various networks shown in Figs. 18(a), 19(a), and 20(a), where the controller gain $k_i\ \forall\, i$ are the same as the previous experiment. The initial conditions (17) are changed to $\theta_1(0) = -37.8$, $\theta_2(0) = -27.7$, $\theta_3(0) = 43.1$, $\theta_4(0) = 20.0$ in order to guarantee that the relative orientation matrices are positive definite. The experimental results are shown in Figs. 18(b), 19(b), and 20(b), which illustrate the orientations of the rigid bodies. The graph structure in Figs. 19 and 20 achieves faster convergence than that of Fig. 18. These

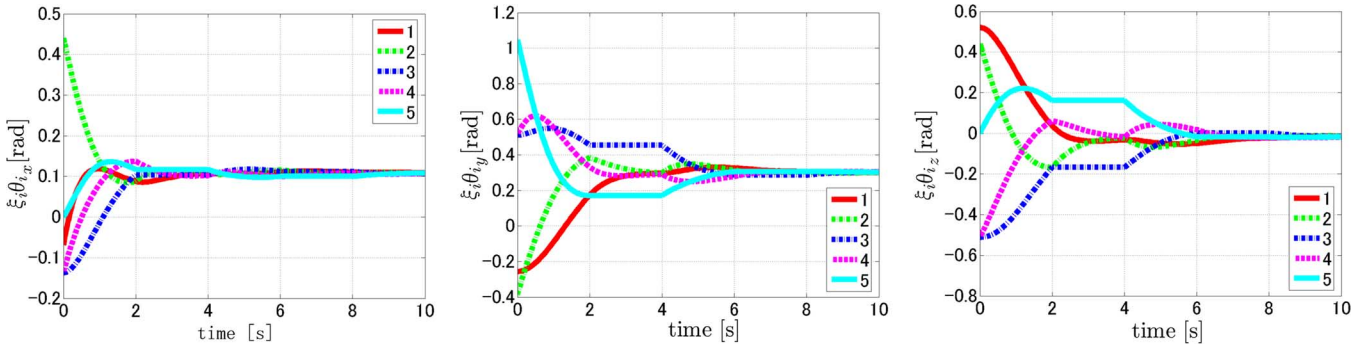

Fig. 10. Time responses of rotation vector $\xi_i\theta_i$ (Simulation 2).

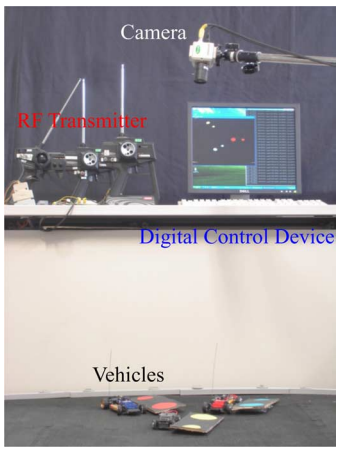

Fig. 11. Experiment environment.

Fig. 12. Vehicles.

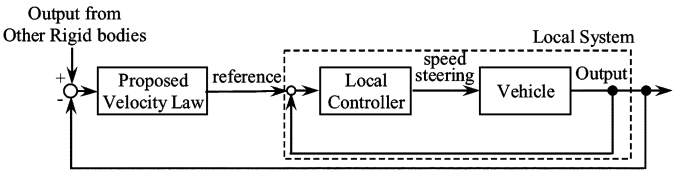

Fig. 13. Local control system.

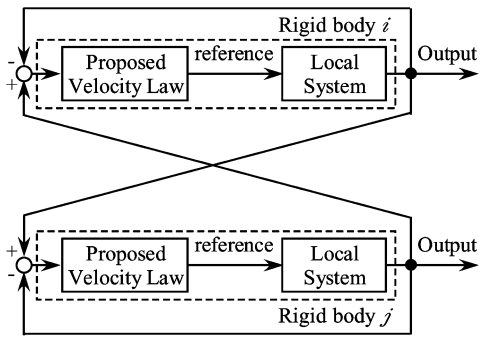

Fig. 14. Total control system.

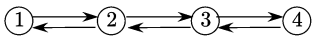

Fig. 15. Graph topology.

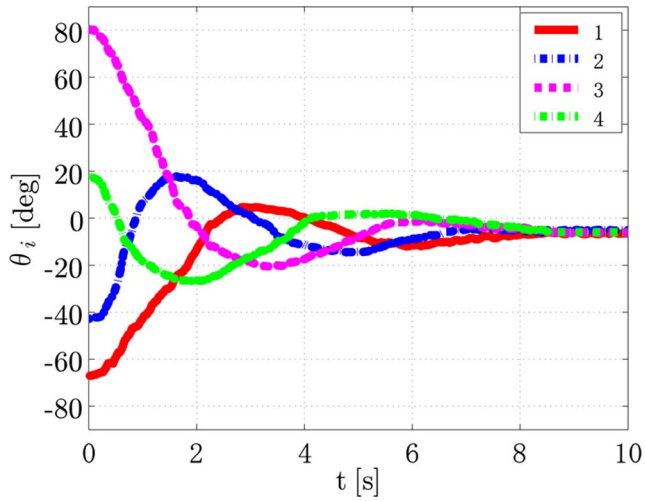

Fig. 16. Time responses of orientation.

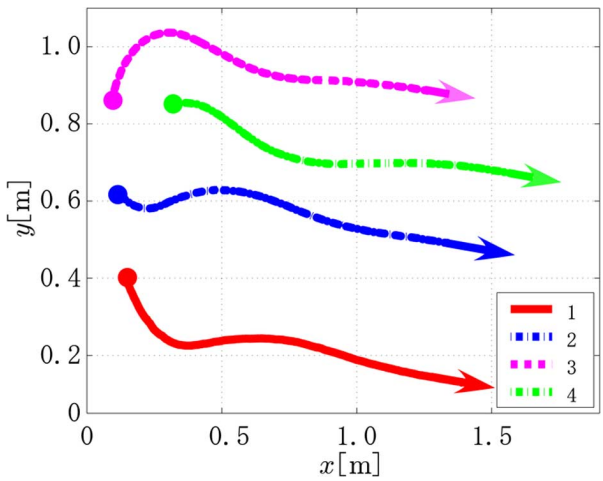

Fig. 17. Time responses of positions.

results suggest that the bigger $\lambda_{\min 2}(L_{\gamma\mathrm{sym}})$ is, the faster convergence is attained as stated in Section IV-A.

VI. Conclusion

In this paper, we have investigated passivity-based attitude synchronization in $SE(3)$ of the kinematics of rigid bodies. We first have developed a passivity-based control law locally

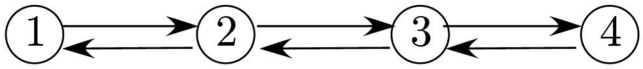

(a) graph 1

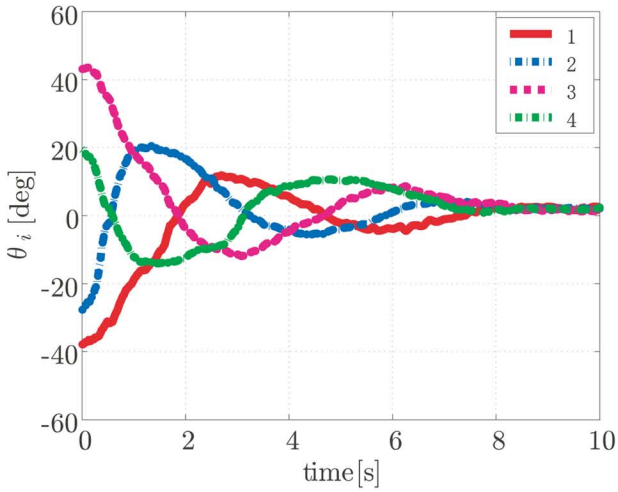

(b)

Fig. 18. Experimental result for graph 1 ($\lambda_{\min 2}(L_{\gamma \mathrm{sym}}) = 1.0$).

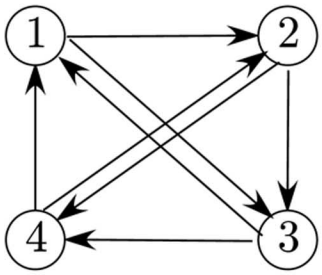

(a) graph 2

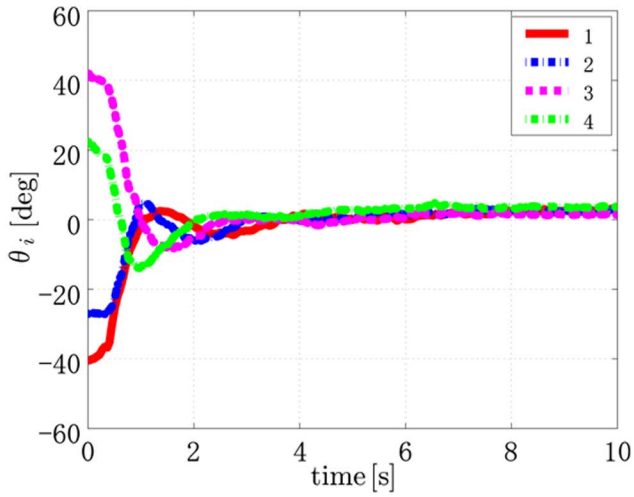

(b)

Fig. 19. Experimental result for graph 2 ($\lambda_{\min 2}(L_{\gamma \mathrm{sym}}) = 2.0$).

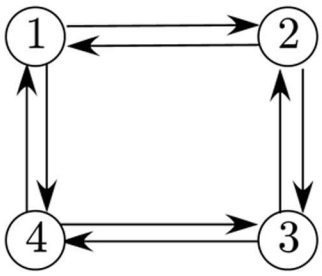

(a) graph 3

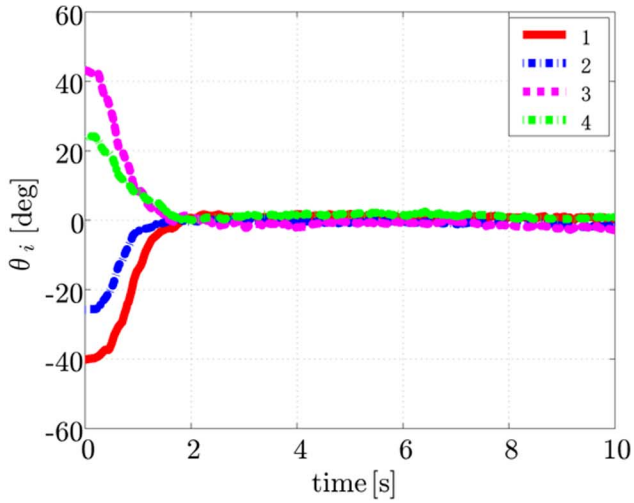

(b)

Fig. 20. Experimental result for graph 3 ($\lambda_{\min 2}(L_{\gamma \mathrm{sym}}) = 2.0$).

attaining attitude synchronization. Passivity has been also employed in connectivity analysis and we have established a connection between the speed of convergence and the graph structure. We have also shown the facts that the passivity-based con-

trol input still attains attitude synchronization in various situations such as the cases with communication delay, a leader and a topology switching. The simulation and experimental results have demonstrated the validity of our results.

A further direction of this research is to extend the results of this paper to pose (position and attitude) synchronization.

APPENDIX A
PROOF OF THEOREM 1

Before proving this theorem, we prepare the following Lemma on properties of the graph Laplacian.

Lemma 3:

1) If the graph is strongly connected and the weights are positive, there exists a vector γ satisfying $\gamma^T L_{\rm w} = 0$ whose elements are positive [9], [46].
2) If the graph is strongly connected, $\mathrm{rank}(L_{\rm w}) = n-1$ [2].

Proof: Define the potential function

$$U_{\rm A} := \sum_{i=1}^{n} \frac{\gamma_i}{k_i}\phi(e^{\hat{\xi}_i\theta_i}), \quad \phi(e^{\hat{\xi}_i\theta_i}) := \frac{1}{2}\mathrm{tr}\left(I - e^{\hat{\xi}_i\theta_i}\right)$$

where $\phi(e^{\hat{\xi}_i\theta_i})$ is the energy function of rotation of rigid body i and γ_i are elements of the vector γ satisfying

$$\gamma^T L_{\rm w} = 0, \quad \gamma^T = [\gamma_1, \ldots, \gamma_n], \quad \gamma_i > 0 \quad \forall\, i \in \{1, \ldots, n\}. \tag{18}$$

From the (2) and (7), the derivative of this potential function along trajectories of the kinematics model (1) is given by

$$\begin{aligned}\dot{U}_{\rm A} &= \sum_{i=1}^{n} \frac{\gamma_i}{k_i}\left(\mathbf{sk}(e^{\hat{\xi}_i\theta_i})^{\vee}\right)^T \omega_i \\ &= \sum_{i=1}^{n}\sum_{j\in\mathcal{N}_i} \gamma_i w_{ij}\left(\mathbf{sk}(e^{\hat{\xi}_i\theta_i})^{\vee}\right)^T \mathbf{sk}(e^{-\hat{\xi}_i\theta_i}e^{\hat{\xi}_j\theta_j})^{\vee}.\end{aligned}$$

From the fact that $a^T b = -1/2\mathrm{tr}(\hat{a}\hat{b})$ holds for any 3-D vectors $a \in \mathcal{R}^3$ and $b \in \mathcal{R}^3$, we next obtain (19), shown at the bottom of the page. Thus, (19) can be rewritten as

$$\begin{aligned}\dot{U}_{\rm A} = \sum_{i=1}^{n}\sum_{j\in\mathcal{N}_i} \gamma_i w_{ij}\Big(&-\phi(e^{\hat{\xi}_i\theta_i}) + \phi(e^{\hat{\xi}_j\theta_j}) \\ &-\frac{1}{4}\mathrm{tr}\left((e^{\hat{\xi}_i\theta_i} + e^{-\hat{\xi}_i\theta_i})(I - e^{-\hat{\xi}_i\theta_i}e^{\hat{\xi}_j\theta_j})\right)\Big).\end{aligned}$$

Since rotation matrices $e^{\hat{\xi}_i\theta_i}\ \forall\, i$ are assumed to be positive definite, the following inequality holds [45]:

$$\begin{aligned}&-\mathrm{tr}\left((e^{\hat{\xi}_i\theta_i} + e^{-\hat{\xi}_i\theta_i})(I - e^{-\hat{\xi}_i\theta_i}e^{\hat{\xi}_j\theta_j})\right) \\ &\qquad \le -\lambda_{\min}(e^{\hat{\xi}_i\theta_i} + e^{-\hat{\xi}_i\theta_i})\mathrm{tr}\left(I - e^{-\hat{\xi}_i\theta_i}e^{\hat{\xi}_j\theta_j}\right)\end{aligned} \tag{20}$$

where $\lambda_{\min}(e^{\hat{\xi}_i\theta_i} + e^{-\hat{\xi}_i\theta_i})$ is a minimal eigenvalue of a matrix $e^{\hat{\xi}_i\theta_i} + e^{-\hat{\xi}_i\theta_i}$. Therefore, the derivative of the potential function satisfies

$$\begin{aligned}\dot{U}_{\rm A} \le \sum_{i=1}^{n}\sum_{j\in\mathcal{N}_i} \gamma_i w_{ij}\Big(&-\phi(e^{\hat{\xi}_i\theta_i}) + \phi(e^{\hat{\xi}_j\theta_j}) \\ &-\frac{1}{2}\lambda_{\min}(e^{\hat{\xi}_i\theta_i} + e^{-\hat{\xi}_i\theta_i})\phi(e^{-\hat{\xi}_i\theta_i}e^{\hat{\xi}_j\theta_j})\Big).\end{aligned}$$

From Lemma 3, the term $\sum_{i=1}^{n}\sum_{j\in\mathcal{N}_i}\gamma_i w_{ij}\left(-\phi(e^{\hat{\xi}_i\theta_i}) + \phi(e^{\hat{\xi}_j\theta_j})\right)$ satisfies

$$\begin{aligned}&\sum_{i=1}^{n}\sum_{j\in\mathcal{N}_i} \gamma_i w_{ij}\left(-\phi(e^{\hat{\xi}_i\theta_i}) + \phi(e^{\hat{\xi}_j\theta_j})\right) \\ &\qquad = -\gamma^T L_{\rm w}\begin{bmatrix}\phi(e^{\hat{\xi}_1\theta_1}) \\ \vdots \\ \phi(e^{\hat{\xi}_n\theta_n})\end{bmatrix} = 0.\end{aligned} \tag{21}$$

$$\begin{aligned}&\left(\mathbf{sk}(e^{\hat{\xi}_i\theta_i})^{\vee}\right)^T \mathbf{sk}(e^{-\hat{\xi}_i\theta_i}e^{\hat{\xi}_j\theta_j})^{\vee} \\ &= -\frac{1}{2}\mathrm{tr}\left(\mathbf{sk}(e^{\hat{\xi}_i\theta_i})\mathbf{sk}(e^{-\hat{\xi}_i\theta_i}e^{\hat{\xi}_j\theta_j})\right) \quad \left(\because a^T b = -\frac{1}{2}\mathrm{tr}(\hat{a}\hat{b})\right) \\ &= -\frac{1}{8}\mathrm{tr}\left((e^{\hat{\xi}_i\theta_i} - e^{-\hat{\xi}_i\theta_i})(e^{-\hat{\xi}_i\theta_i}e^{\hat{\xi}_j\theta_j} - e^{-\hat{\xi}_j\theta_j}e^{\hat{\xi}_i\theta_i})\right) \quad \left(\because \mathbf{sk}(e^{\hat{\xi}_i\theta_i}) := \frac{1}{2}(e^{\hat{\xi}_i\theta_i} - e^{-\hat{\xi}_i\theta_i})\right) \\ &= -\frac{1}{8}\mathrm{tr}\left(e^{\hat{\xi}_j\theta_j} - e^{\hat{\xi}_i\theta_i}e^{-\hat{\xi}_j\theta_j}e^{\hat{\xi}_i\theta_i} - e^{-\hat{\xi}_i\theta_i}e^{-\hat{\xi}_i\theta_i}e^{\hat{\xi}_j\theta_j} + e^{-\hat{\xi}_i\theta_i}e^{-\hat{\xi}_j\theta_j}e^{\hat{\xi}_i\theta_i}\right) \\ &= -\frac{1}{4}\mathrm{tr}\left(e^{\hat{\xi}_j\theta_j} - e^{-2\hat{\xi}_i\theta_i}e^{\hat{\xi}_j\theta_j}\right) \quad (\because \mathrm{tr}(A) = \mathrm{tr}(A^T),\ \mathrm{tr}(AB) = \mathrm{tr}(BA)) \\ &= -\frac{1}{4}\mathrm{tr}\left(2I - 2e^{\hat{\xi}_i\theta_i} - 2I + 2e^{\hat{\xi}_j\theta_j} + (e^{\hat{\xi}_i\theta_i} + e^{-\hat{\xi}_i\theta_i})(I - e^{-\hat{\xi}_i\theta_i}e^{\hat{\xi}_j\theta_j})\right) \\ &= -\phi(e^{\hat{\xi}_i\theta_i}) + \phi(e^{\hat{\xi}_j\theta_j}) - \frac{1}{4}\mathrm{tr}\left((e^{\hat{\xi}_i\theta_i} + e^{-\hat{\xi}_i\theta_i})(I - e^{-\hat{\xi}_i\theta_i}e^{\hat{\xi}_j\theta_j})\right) \quad \left(\because \phi(e^{\hat{\xi}_i\theta_i}) := \frac{1}{2}\mathrm{tr}(I - e^{\hat{\xi}_i\theta_i})\right)\end{aligned} \tag{19}$$

This yields the following inequality, and hence the deviation of the potential function is nonpositive definite:

$$\dot{U}_{\mathrm{A}} \leq -\frac{1}{2}\sum_{i=1}^{n}\sum_{j\in\mathcal{N}_i}\gamma_i w_{ij}\lambda_{\min} \times(e^{\hat{\xi}_i\theta_i}+e^{-\hat{\xi}_i\theta_i})\phi(e^{-\hat{\xi}_i\theta_i}e^{\hat{\xi}_j\theta_j})\leq 0. \quad (22)$$

The inequality (22) means the potential function U_{A} is non-increasing for all $t\geq 0$. Let us now define the set $E_{\mathrm{A}}=\{e^{\hat{\xi}_i\theta_i}\in SO(3), \forall i \mid e^{\hat{\xi}_i\theta_i}>0\, \dot{U}_{\mathrm{A}}\equiv 0\}$. Then, the set E_{A} is characterized by all trajectories satisfying $\phi(e^{-\hat{\xi}_i\theta_i}e^{\hat{\xi}_j\theta_j})\equiv 0\,\forall\, j\in\mathcal{N}_i$, $\forall i$. Therefore, Lasalle's Invariance Principle [47] and strong connectivity of the information graph prove attitude synchronization of (5). ■

Appendix B
Proof of Lemma 2

In this proof, we use the fact that the positive definiteness of the rotation matrix $e^{\hat{\xi}_i\theta_i}$ is equivalent to $\phi(e^{\hat{\xi}_i\theta_i})<1$.

Let $\alpha(t)\in\{1,\ldots,n\}, t\geq 0$ denote the rigid body with the maximal energy function at time t, i.e.,

$$\alpha(t):=\arg\max_{i\in\{1,\ldots,n\}}\phi(e^{\hat{\xi}_i\theta_i(t)}).$$

Then, the derivative of this potential function $\phi(e^{\hat{\xi}_\alpha\theta_\alpha})$ along the trajectory of the kinematics model (1) is given by

$$\begin{aligned}\dot{\phi}(e^{\hat{\xi}_\alpha\theta_\alpha}) &= \left(\mathbf{sk}(e^{\hat{\xi}_\alpha\theta_\alpha})^\vee\right)^T\omega_\alpha\\ &= \left(\mathbf{sk}(e^{\hat{\xi}_\alpha\theta_\alpha})^\vee\right)^T\sum_{j\in\mathcal{N}_\alpha}k_\alpha\omega_{\alpha j}\mathbf{sk}(e^{-\hat{\xi}_\alpha\theta_\alpha}e^{\hat{\xi}_j\theta_j})^\vee\\ &= \sum_{j\in\mathcal{N}_\alpha}k_\alpha\omega_{\alpha j}\left(\mathbf{sk}(e^{\hat{\xi}_\alpha\theta_\alpha})^\vee\right)^T\mathbf{sk}(e^{-\hat{\xi}_\alpha\theta_\alpha}e^{\hat{\xi}_j\theta_j})^\vee.\end{aligned}$$

Calculations similar to (19) and (20) yields the inequality

$$\dot{\phi}(e^{\hat{\xi}_\alpha\theta_\alpha})\leq\sum_{j\in\mathcal{N}_\alpha}k_\alpha\omega_{\alpha j}\Big(-\phi(e^{\hat{\xi}_\alpha\theta_\alpha})+\phi(e^{\hat{\xi}_j\theta_j}) -\frac{1}{2}\lambda_{\min}(e^{\hat{\xi}_\alpha\theta_\alpha}+e^{-\hat{\xi}_\alpha\theta_\alpha})\phi(e^{-\hat{\xi}_\alpha\theta_\alpha}e^{\hat{\xi}_j\theta_j})\Big).$$

It is clear from the definition of α that

$$-\phi(e^{\hat{\xi}_\alpha\theta_\alpha})+\phi(e^{\hat{\xi}_j\theta_j})\leq 0\,\forall\, j.$$

Since $\lambda_{\min}(e^{\hat{\xi}_\alpha\theta_\alpha}+e^{-\hat{\xi}_\alpha\theta_\alpha})\phi(I-e^{-\hat{\xi}_\alpha\theta_\alpha}e^{\hat{\xi}_j\theta_j})\geq 0$, the inequality $\dot{\phi}(e^{\hat{\xi}_\alpha\theta_\alpha})\leq 0$ holds true. We thus obtain

$$\begin{aligned}\phi(e^{\hat{\xi}_i(t)\theta_i(t)})&\leq\phi(e^{\hat{\xi}_\alpha(t)\theta_\alpha(t)})\\ &\leq\phi(e^{\hat{\xi}_\alpha(0)\theta_\alpha(0)})<1\\ &\forall i\in\{1,\ldots,n\},\quad t\geq 0\end{aligned}$$

from the assumption that the rotation matrices are positive definite at the initial time. This inequality implies that all the rigid bodies' orientation matrices are positive definite for any time $t\geq 0$. This completes the proof.

Appendix C
Proof of Theorem 2

Before proving this theorem, we present the following lemmas.

Lemma 4: Define the function

$$\tilde{U}_{\exp}:=2\sum_{i=1}^{n}\sum_{l=1}^{n}\frac{\gamma_i\gamma_l}{k_ik_l}\phi(e^{-\hat{\xi}_i\theta_i}e^{\hat{\xi}_l\theta_l})$$

where γ_i and γ_l are given by (18). Then, $\tilde{U}_{\exp}$ satisfies the inequality

$$\min_{i,l}\frac{\gamma_i\gamma_l}{k_ik_l}U_{\exp}\leq\tilde{U}_{\exp}\leq\max_{i,l}\frac{\gamma_i\gamma_l}{k_ik_l}U_{\exp}. \quad (23)$$

Proof: By the definition of $U_{\exp}$ and $\tilde{U}_{\exp}$, we immediately obtain

$$\begin{aligned}\min_{i,l}\frac{\gamma_i\gamma_l}{k_ik_l}\sum_{i=1}^{n}\sum_{l=1}^{n}2\phi(e^{-\hat{\xi}_i\theta_i}e^{\hat{\xi}_l\theta_l})&\\ \leq\tilde{U}_{\exp}\leq\max_{i,l}\frac{\gamma_i\gamma_l}{k_ik_l}\sum_{i=1}^{n}\sum_{l=1}^{n}2\phi(e^{-\hat{\xi}_i\theta_i}e^{\hat{\xi}_l\theta_l})&\end{aligned} \quad (24)$$

and

$$\begin{aligned}\sum_{i=1}^{n}\sum_{l=1}^{n}2\phi(e^{-\hat{\xi}_i\theta_i}e^{\hat{\xi}_l\theta_l})&=\mathrm{tr}\left((e^{\hat{\xi}\theta})^T(M\otimes I_3)e^{\hat{\xi}\theta}\right)\\ &=U_{\exp}.\end{aligned} \quad (25)$$

Thus, (23) follows from (24) and (25). ■

Lemma 5: There exists an $\epsilon>0$ satisfying

$$\dot{\tilde{U}}_{\exp}\leq-\frac{\epsilon}{n}\lambda_{\min 2}(L_{\gamma\mathrm{sym}}) \times\sum_{l=1}^{n}\frac{\gamma_l}{k_l}\mathrm{tr}\left((e^{\hat{\xi}\theta})^T(M\otimes I_3)e^{\hat{\xi}\theta}\right). \quad (26)$$

Proof: The derivative of $\tilde{U}_{\exp}$ along trajectories of (1) is given by in (27), shown at the bottom of the next page. Making a calculation similar to (21), we obtain

$$\sum_{i=1}^{n}\sum_{j\in\mathcal{N}_i}\gamma_i w_{ij}e^{\hat{\xi}_j\theta_j}=\sum_{i=1}^{n}\sum_{j\in\mathcal{N}_i}\gamma_i w_{ij}e^{\hat{\xi}_i\theta_i}. \quad (28)$$

It follows from (28) that

$$\begin{aligned}\sum_{l=1}^{n}\frac{\gamma_l}{k_l}\sum_{i=1}^{n}\sum_{j\in\mathcal{N}_i}\gamma_i w_{ij}e^{-\hat{\xi}_l\theta_l}e^{\hat{\xi}_j\theta_j}&\\ =\sum_{l=1}^{n}\frac{\gamma_l}{k_l}\sum_{i=1}^{n}\sum_{j\in\mathcal{N}_i}\gamma_i w_{ij}e^{-\hat{\xi}_l\theta_l}e^{\hat{\xi}_i\theta_i}&\end{aligned} \quad (29)$$

and from (29)

$$\begin{aligned}\sum_{l=1}^{n}\frac{\gamma_l}{k_l}\sum_{i=1}^{n}\sum_{j\in\mathcal{N}_i}\gamma_i w_{ij}\mathrm{tr}\left(e^{-\hat{\xi}_l\theta_l}e^{\hat{\xi}_i\theta_i}(e^{-\hat{\xi}_i\theta_i}e^{\hat{\xi}_j\theta_j}-I)\right)\\ =\sum_{l=1}^{n}\frac{\gamma_l}{k_l}\sum_{i=1}^{n}\sum_{j\in\mathcal{N}_i}\gamma_i w_{ij}\mathrm{tr}\left(e^{-\hat{\xi}_i\theta_l}e^{\hat{\xi}_j\theta_j}-e^{-\hat{\xi}_l\theta_l}e^{\hat{\xi}_i\theta_i}\right)\\ =0\end{aligned}\tag{30}$$

holds true. Hence, we have (31), shown at the bottom of the page. Since the rotation matrices $e^{-\hat{\xi}_i\theta_i}e^{\hat{\xi}_j\theta_j}\ \forall\, i,j$ are assumed to be positive definite, they satisfy the following inequality [45]:

$$\begin{aligned}&-\mathrm{tr}\left((e^{-\hat{\xi}_i\theta_i}e^{\hat{\xi}_l\theta_l}+e^{-\hat{\xi}_l\theta_l}e^{\hat{\xi}_i\theta_i})(I-e^{-\hat{\xi}_i\theta_i}e^{\hat{\xi}_j\theta_j})\right)\\ &\quad\le-\lambda_{\min}(e^{-\hat{\xi}_i\theta_i}e^{\hat{\xi}_l\theta_l}+e^{-\hat{\xi}_l\theta_l}e^{\hat{\xi}_i\theta_i})\mathrm{tr}\left(I-e^{-\hat{\xi}_i\theta_i}e^{\hat{\xi}_j\theta_j}\right).\end{aligned}\tag{32}$$

Substituting the inequality (32) into (31) yields

$$\begin{aligned}\dot{\tilde{U}}_{\exp}\le&-\sum_{l=1}^{n}\frac{\gamma_l}{k_l}\sum_{i=1}^{n}\sum_{j\in\mathcal{N}_i}\gamma_i w_{ij}\\ &\times\lambda_{\min}(e^{-\hat{\xi}_i\theta_i}e^{\hat{\xi}_l\theta_l}+e^{-\hat{\xi}_l\theta_l}e^{\hat{\xi}_i\theta_i})\mathrm{tr}\left(I-e^{-\hat{\xi}_i\theta_i}e^{\hat{\xi}_j\theta_j}\right).\end{aligned}\tag{33}$$

Let us now define

$$\epsilon:=\min_{i,l,t}\lambda_{\min}(e^{-\hat{\xi}_i(t)\theta_i(t)}e^{\hat{\xi}_l(t)\theta_l(t)}+e^{-\hat{\xi}_l(t)\theta_l(t)}e^{\hat{\xi}_i(t)\theta_i(t)}).$$

Then, $\epsilon > 0$ because of the assumption that $e^{-\hat{\xi}_i(t)\theta_i(t)}e^{\hat{\xi}_j(t)\theta_j(t)}$ are positive definite for all i and j. From this definition, (33) can be rewritten as (34), shown at

---

$$\begin{aligned}\dot{\tilde{U}}_{\exp}=&2\sum_{i=1}^{n}\sum_{l=1}^{n}\frac{\gamma_i\gamma_l}{k_ik_l}\left(\mathbf{sk}(e^{-\hat{\xi}_i\theta_i}e^{\hat{\xi}_l\theta_l})^{\vee}\right)^{T}(-\omega_i+\omega_l)\\ =&-4\sum_{i=1}^{n}\sum_{l=1}^{n}\frac{\gamma_i\gamma_l}{k_ik_l}\left(\mathbf{sk}(e^{-\hat{\xi}_i\theta_i}e^{\hat{\xi}_l\theta_l})^{\vee}\right)^{T}\omega_i\\ =&-4\sum_{i=1}^{n}\sum_{l=1}^{n}\sum_{j\in\mathcal{N}_i}\frac{\gamma_i\gamma_l}{k_l}w_{ij}\left(\mathbf{sk}(e^{-\hat{\xi}_i\theta_i}e^{\hat{\xi}_l\theta_l})^{\vee}\right)^{T}\mathbf{sk}(e^{-\hat{\xi}_i\theta_i}e^{\hat{\xi}_j\theta_j})^{\vee}\\ =&2\sum_{i=1}^{n}\sum_{l=1}^{n}\sum_{j\in\mathcal{N}_i}\frac{\gamma_i\gamma_l}{k_l}w_{ij}\mathrm{tr}\left(\mathbf{sk}(e^{-\hat{\xi}_i\theta_i}e^{\hat{\xi}_l\theta_l})\mathbf{sk}(e^{-\hat{\xi}_i\theta_i}e^{\hat{\xi}_j\theta_j})\right)\quad\left(\because a^Tb=-\frac{1}{2}\mathrm{tr}(\hat{a}\hat{b})\right)\\ =&\frac{1}{2}\sum_{i=1}^{n}\sum_{l=1}^{n}\sum_{j\in\mathcal{N}_i}\frac{\gamma_i\gamma_l}{k_l}w_{ij}\mathrm{tr}\left((e^{-\hat{\xi}_i\theta_i}e^{\hat{\xi}_l\theta_l}-e^{-\hat{\xi}_l\theta_l}e^{\hat{\xi}_i\theta_i})(e^{-\hat{\xi}_i\theta_i}e^{\hat{\xi}_j\theta_j}-e^{-\hat{\xi}_j\theta_j}e^{\hat{\xi}_i\theta_i})\right)\\ =&\sum_{l=1}^{n}\frac{\gamma_l}{k_l}\sum_{i=1}^{n}\sum_{j\in\mathcal{N}_i}\gamma_i w_{ij}\mathrm{tr}\left(e^{-\hat{\xi}_i\theta_i}e^{\hat{\xi}_l\theta_l}e^{-\hat{\xi}_i\theta_i}e^{\hat{\xi}_j\theta_j}-e^{-\hat{\xi}_l\theta_l}e^{\hat{\xi}_j\theta_j}\right).\end{aligned}\tag{27}$$

$$\begin{aligned}\dot{\tilde{U}}_{\exp}=&\sum_{l=1}^{n}\frac{\gamma_l}{k_l}\sum_{i=1}^{n}\sum_{j\in\mathcal{N}_i}\gamma_i w_{ij}\mathrm{tr}\left(e^{-\hat{\xi}_i\theta_i}e^{\hat{\xi}_l\theta_l}e^{-\hat{\xi}_i\theta_i}e^{\hat{\xi}_j\theta_j}-e^{-\hat{\xi}_l\theta_l}e^{\hat{\xi}_i\theta_i}\right)\quad(\because(29))\\ =&\sum_{l=1}^{n}\frac{\gamma_l}{k_l}\sum_{i=1}^{n}\sum_{j\in\mathcal{N}_i}\gamma_i w_{ij}\mathrm{tr}\left(e^{-\hat{\xi}_i\theta_i}e^{\hat{\xi}_l\theta_l}(e^{-\hat{\xi}_i\theta_i}e^{\hat{\xi}_j\theta_j}-I)\right)\\ =&\sum_{l=1}^{n}\frac{\gamma_l}{k_l}\sum_{i=1}^{n}\sum_{j\in\mathcal{N}_i}\gamma_i w_{ij}\mathrm{tr}\left(e^{-\hat{\xi}_i\theta_i}e^{\hat{\xi}_l\theta_l}(e^{-\hat{\xi}_i\theta_i}e^{\hat{\xi}_j\theta_j}-I)\right)\\ &+\sum_{l=1}^{n}\frac{\gamma_l}{k_l}\sum_{i=1}^{n}\sum_{j\in\mathcal{N}_i}\gamma_i w_{ij}\mathrm{tr}\left(e^{-\hat{\xi}_l\theta_l}e^{\hat{\xi}_i\theta_i}(e^{-\hat{\xi}_i\theta_i}e^{\hat{\xi}_j\theta_j}-I)\right)\quad(\because(30))\\ =&\sum_{l=1}^{n}\frac{\gamma_l}{k_l}\sum_{i=1}^{n}\sum_{j\in\mathcal{N}_i}\gamma_i w_{ij}\mathrm{tr}\left((e^{-\hat{\xi}_i\theta_i}e^{\hat{\xi}_l\theta_l}+e^{-\hat{\xi}_l\theta_l}e^{\hat{\xi}_i\theta_i})(e^{-\hat{\xi}_i\theta_i}e^{\hat{\xi}_j\theta_j}-I)\right)\\ =&-\sum_{l=1}^{n}\frac{\gamma_l}{k_l}\sum_{i=1}^{n}\sum_{j\in\mathcal{N}_i}\gamma_i w_{ij}\mathrm{tr}\left((e^{-\hat{\xi}_i\theta_i}e^{\hat{\xi}_l\theta_l}+e^{-\hat{\xi}_l\theta_l}e^{\hat{\xi}_i\theta_i})(I-e^{-\hat{\xi}_i\theta_i}e^{\hat{\xi}_j\theta_j})\right).\end{aligned}\tag{31}$$

the bottom of the page. Due to a property of the Kronecker product, $\mathbf{1}^T(M\otimes I_3)e^{\hat{\xi}\theta}x = 0\ \forall\ x$ and the Courant-Fischer theorem [46], the following inequality is satisfied:

$$\lambda_{\min 2}(L_{\gamma\mathrm{sym}})x^T(e^{\hat{\xi}\theta})^T(M\otimes I_3)(M\otimes I_3)e^{\hat{\xi}\theta}x \le x^T(e^{\hat{\xi}\theta})^T(M\otimes I_3)(L_{\gamma\mathrm{sym}}\otimes I_3)(M\otimes I_3)e^{\hat{\xi}\theta}x.$$

This implies that $(e^{\hat{\xi}\theta})^T(M\otimes I_3)((L_{\gamma\mathrm{sym}}-\lambda_{\min 2}(L_{\gamma\mathrm{sym}})I)\otimes I_3)(M\otimes I_3)e^{\hat{\xi}\theta}$ is semipositive definite, and that

$$\begin{aligned}&-\mathrm{tr}\left((e^{\hat{\xi}\theta})^T(M\otimes I_3)(L_{\gamma\mathrm{sym}}\otimes I_3)(M\otimes I_3)e^{\hat{\xi}\theta}\right)\\ &\le -\lambda_{\min 2}(L_{\gamma\mathrm{sym}})\mathrm{tr}\left((e^{\hat{\xi}\theta})^T(M\otimes I_3)(M\otimes I_3)e^{\hat{\xi}\theta}\right)\\ &= -n\lambda_{\min 2}(L_{\gamma\mathrm{sym}})\mathrm{tr}\left((e^{\hat{\xi}\theta})^T(M\otimes I_3)e^{\hat{\xi}\theta}\right)\\ &\quad(\because MM=nM).\end{aligned}\tag{35}$$

The inequality (26) now follows from the inequalities (34) and (35). ■

Now, we are ready to prove Theorem 2.

Proof: From Lemmas 4 and 5, we get

$$\begin{aligned}\dot{\tilde{U}}_{\exp} &\le -\frac{\epsilon}{n}\lambda_{\min 2}(L_{\gamma\mathrm{sym}})\frac{1}{\max_{i,l}\frac{\gamma_i\gamma_l}{k_ik_l}}\sum_{l=1}^{n}\frac{\gamma_l}{k_l}\tilde{U}_{\exp}\\ &= -\frac{\epsilon}{n}\lambda_{\min 2}(L_{\gamma\mathrm{sym}})\min_{i,l}\frac{k_ik_l}{\gamma_i\gamma_l}\sum_{l=1}^{n}\frac{\gamma_l}{k_l}\tilde{U}_{\exp}.\end{aligned}$$

It follows from the comparison principle [47] that

$$\tilde{U}_{\exp}\le\tilde{U}_{\exp}(0)e^{-\epsilon/n\lambda_{\min 2}(L_{\gamma\mathrm{sym}})\min_{i,l}k_ik_l/\gamma_i\gamma_l\sum_{l=1}^{n}\gamma_l/k_lt}.\tag{36}$$

The inequalities (23) and (36) together imply the inequality (37), shown at the bottom of the page. The proof is thus completed taking:

- $a_e := \max_{i,l}\gamma_i\gamma_l/k_ik_l/\min_{i,l}\gamma_i\gamma_l/k_ik_l > 0$;
- $b_e := \epsilon/n\min_{i,l}k_ik_l/\gamma_i\gamma_l\sum_{l=1}^{n}\gamma_l/k_l > 0$;
- $\epsilon := \min_{i,l,t}\lambda_{\min}(e^{-\hat{\xi}_i(t)\theta_i(t)}e^{\hat{\xi}_l(t)\theta_l(t)} + e^{-\hat{\xi}_l(t)\theta_l(t)}e^{\hat{\xi}_i(t)\theta_i(t)})$.

■

Appendix D
Proof of Theorem 3

Proof: From Lemma 3 in Appendix A it follows that if $s(t)\in\mathcal{G}_{\mathrm{dc}}$, then the algebraic connectivity satisfies $\lambda_{\min 2}(L_{\gamma\mathrm{sym}}(s(t))) = 0$ and $\lambda_{\min 2}(L_{\gamma\mathrm{sym}}(s(t))) > 0$ otherwise. By using the characteristic function, the inequality (15) can be rewritten on the interval $[t,t_i)$ as

$$U_{\exp}(t)\le a_e^*U_{\exp}(t_i)e^{-\lambda^*(1-\mathcal{X}(s(t)))(t-t_i)}\tag{38}$$

where $a_e^* := \min_{s(t)\in\mathcal{G}}a_e$, $\lambda^* := \min_{s(t)\in\mathcal{G}_c}\lambda_{\min 2(L_{\gamma\mathrm{sym}})}b_e$, and a_e, b_e, ϵ are defined in the proof of Theorem 2 (Appendix B). The inequality (38) implies that

$$U_{\exp}(t)\le a_e^*U_{\exp}(t_i)e^{-\lambda^*(t-t_i-T(t_i,t))}\tag{39}$$

holds true on the interval $[t,t_i)$, where $T(t_i,t) := \int_{t_i}^{t}\mathcal{X}(s(r))dr = \mathcal{X}(s(t))(t-t_i)$. Similarly, it follows from (15) that the function $U_{\exp}$ satisfies

$$U_{\exp}(t_i)\le a_e^*U_{\exp}(t_{i-1})e^{-\lambda^*(t_i-t_{i-1}-T(t_{i-1},t_i))}\tag{40}$$

on the interval $[t_i,t_{i-1})$. Substituting (40) to (39) yields the inequality

$$U_{\exp}(t)\le(a_e^*)^2U_{\exp}(t_{i-1})e^{-\lambda^*(t-t_{i-1}-T(t_{i-1},t))}.$$

By iterating the above calculation, we obtain

$$\begin{aligned}U_{\exp}(t)&\le(a_e^*)^{N_s(0,t)}U_{\exp}(0)e^{-\lambda^*(t-T(0,t))}\\ &= U_{\exp}(0)e^{-\lambda^*(t-T(0,t))+\ln(a_e^*)^{N_s(0,t)}}\\ &= U_{\exp}(0)e^{-\lambda^*(t-T(0,t))+N_s(0,t)\ln(a_e^*)}\end{aligned}$$

$$\begin{aligned}\dot{\tilde{U}}_{\exp} &\le -\epsilon\sum_{l=1}^{n}\frac{\gamma_l}{k_l}\sum_{i=1}^{n}\sum_{j\in\mathcal{N}_i}\gamma_iw_{ij}\mathrm{tr}\left(I-e^{-\hat{\xi}_i\theta_i}e^{\hat{\xi}_j\theta_j}\right)\\ &= -\epsilon\sum_{l=1}^{n}\frac{\gamma_l}{k_l}\mathrm{tr}\left((e^{\hat{\xi}\theta})^T(L_\gamma\otimes I_3)e^{\hat{\xi}\theta}\right)\\ &= -\frac{\epsilon}{n^2}\sum_{l=1}^{n}\frac{\gamma_l}{k_l}\mathrm{tr}\left((e^{\hat{\xi}\theta})^T(ML_\gamma M\otimes I_3)e^{\hat{\xi}\theta}\right)\\ &\quad(\because ML_\gamma M=n^2L_\gamma)\\ &= -\frac{\epsilon}{n^2}\sum_{l=1}^{n}\frac{\gamma_l}{k_l}\mathrm{tr}\left((e^{\hat{\xi}\theta})^T(ML_{\gamma\mathrm{sym}}M\otimes I_3)e^{\hat{\xi}\theta}\right).\end{aligned}\tag{34}$$

$$U_{\exp}\le\frac{\max_{i,l}\frac{\gamma_i\gamma_l}{k_ik_l}}{\min_{i,l}\frac{\gamma_i\gamma_l}{k_ik_l}}U_{\exp}(0)e^{-\lambda_{\min 2}(L_{\gamma\mathrm{sym}})\epsilon/n\min_{i,l}k_ik_l/\gamma_i\gamma_l\sum_{l=1}^{n}\gamma_l/k_lt}.\tag{37}$$

where $N_s(\tau, t)$ denotes the number of graph switches over the interval (τ, t). From the assumptions of the theorem, $T(\tau, t) \leq \alpha(t-\tau) + T_0$ and $N_s(0, t) \leq t/\tau_D$ are satisfied and hence

$$\begin{aligned} U_{\exp}(t) &\leq U_{\exp}(0) e^{-\lambda^*(t-\alpha t+T_0)+\ln(a_e^*)/\tau_D t} \\ &= U_{\exp}(0) e^{(-\lambda^*(1-\alpha)+\ln(a_e^*)/\tau_D)t-\lambda^* T_0}. \end{aligned}$$

This inequality implies that when $-\lambda^*(1-\alpha)+\ln(a_e^*)/\tau_D < 0$ is satisfied, then we have

$$\lim_{t\to\infty} U_{\exp}(t) = 0 \tag{41}$$

which is a necessary and sufficient condition for attitude synchronization. Thus a sufficient conditions for (41) is given by

$$\tau_D > \frac{\ln a_e^*}{\lambda^*(1-\alpha)}$$

which means the existence of a lower bound of τ_D to achieve attitude synchronization. This completes the proof. ■

ACKNOWLEDGMENT

The authors would like to thank Mr. N. Kobayashi for invaluable help in carrying out the experiments.

REFERENCES

[1] *Cooperative Control: A Post-Workshop Volume 2003 Block Island Workshop On Cooperative Control*, ser. Lecture Notes in Control and Information Sciences, V. Kumar, N. Leonard, and A. S. Morse, Eds.. New York: Springer-Verlag, 2004, vol. 309.

[2] R. Olfati-Saber, J. A. Fax, and R. M. Murray, "Consensus and cooperation in networked multi-agent systems," *Proc. IEEE*, vol. 95, no. 1, pp. 215–233, Jan. 2007.

[3] J. Cortes, S. Martinez, T. Karatas, and F. Bullo, "Coverage control for mobile sensing networks," *IEEE Trans. Robot. Autom.*, vol. 20, no. 2, pp. 243–255, Apr. 2004.

[4] W. Li and C. G. Cassandras, "Distributive cooperative coverage control of sensor networks," in *Proc. 44th Conf. Decision Control*, 2005, pp. 2542–2547.

[5] S. Martinez, F. Bullo, J. Cortes, and E. Frazzoli, "On synchronous robotic networks part I: models, tasks and complexity notions," in *Proc. 44th Conf. Decision Control*, 2005, pp. 2847–2856.

[6] S. Martinez, F. Bullo, J. Cortes, and E. Frazzoli, "On synchronous robotic networks part ii: Time complexity of rendezvous and deployment algorithms," in *Proc. 44th IEEE Conf. Decision Control*, 2005, pp. 8313–8318.

[7] W. Ren, "Consensus strategies for cooperative control of vehicle formations," *IET Control Theory Appl.*, vol. 1, no. 2, pp. 505–512, 2007.

[8] S. Martinez, J. Cortes, and F. Bullo, "Motion coordination with distributed information," *IEEE Control Syst. Mag.*, vol. 27, no. 4, pp. 75–88, Apr. 2007.

[9] W. Ren and E. Atkins, "Distributed multi-vehicle coordinated control via Local Information Exchange," *Int. J. Robust Nonlinear Control*, vol. 17, no. 10–11, pp. 1002–1033, 2007.

[10] W. Ren, "Synchronized multiple spacecraft rotations: A revisit in the context of consensus building," in *Proc. Amer. Control Conf.*, 2007, pp. 3174–3179.

[11] J. R. Lawton and R. W. Beard, "Synchronized multiple spacecraft rotations," *Automatica*, vol. 38, no. 8, pp. 1359–1364, 2002.

[12] A. Jadbabaie, J. Lin, and A. S. Morse, "Coordination of groups of mobile autonomous agents using nearest neighbor rules," *IEEE Trans. Autom. Control*, vol. 48, no. 6, pp. 988–1001, Jun. 2003.

[13] H. Tanner, A. Jadbabaie, and G. J. Pappas, "Flocking in fixed and switching networks," *IEEE Trans. Autom. Control*, vol. 52, no. 5, pp. 863–868, May 2007.

[14] N. Moshtagh and A. Jadbabaie, "Distributed geodesic control laws for flocking of nonholonomic agents," *IEEE Trans. Autom. Control*, vol. 52, no. 4, pp. 681–686, Apr. 2007.

[15] R. Olfati-Saber, "Flocking for multi-agent dynamic systems: Algorithms and theory," *IEEE Trans. Autom. Control*, vol. 51, no. 3, pp. 401–420, Mar. 2006.

[16] D. J. Lee and M. W. Spong, "Stable flocking of multiple inertial agents on balanced graphs," *IEEE Trans. Autom. Control*, vol. 52, no. 8, pp. 1469–1475, Aug. 2007.

[17] N. Chopra and M. W. Spong, "On synchronization of kuramoto oscillators," in *Proc. 44th IEEE Conf. Decision Control*, 2005, pp. 3916–3922.

[18] A. Jadbabaie, N. Motee, and M. Barahona, "On the stability of the Kuramoto model of coupled nonlinear oscillators," in *Proc. Amer. Control Conf.*, 2004, pp. 4296–4301.

[19] R. Sepulchre, D. A. Paley, and N. E. Leonard, "Stabilization of planar collective motion: All-to-All communication," *IEEE Trans. Autom. Control*, vol. 52, no. 5, pp. 811–824, May 2007.

[20] A. Sarlette, R. Sepulchre, and N. E. Leonard, "Autonomous rigid body attitude synchronization," in *Proc. 46th IEEE Conf. Decision Control*, 2007, pp. 2566–2571.

[21] A. Sarlette and R. Sepulchre, "Consensus optimization on manifolds," *SIAM J. Control Opt.*, 2008, accepted for publication.

[22] S. Nair and N. E. Leonard, "Stable synchronization of rigid body networks," *Netw. Heterogeneous Media*, vol. 2, no. 4, pp. 595–624, 2007.

[23] D. Bauso, L. Giarré, and R. Pesenti, "Non-linear protocols for optimal distributed consensus in networks of dynamic agents," *Syst. Control Lett.*, vol. 55, no. 11, pp. 918–928, 2006.

[24] N. Chopra and M. W. Spong, "Output synchronization of nonlinear systems with time delay in communication," in *Proc. 45th IEEE Conf. Decision Control*, 2006, pp. 4986–4992.

[25] N. Chopra and M. W. Spong, "Passivity-based control of multi-agent systems," in *Advances in Robot Control: From Everyday Physics to Human-Like Movements*, S. Kawamura and M. Svnin, Eds. New York: Springer, 2006, pp. 107–134.

[26] M. Arcak, "Passivity as a design tool for group coordination," *IEEE Trans. Autom. Control*, vol. 52, no. 8, pp. 1380–1390, Aug. 2007.

[27] I.-A. F. Ihle, M. Arcak, and T. I. Fossen, "Passivity-based designs for synchronized path following," *Automatica*, vol. 43, no. 9, pp. 1508–1518, 2007.

[28] H. Bai, M. Arcak, and J. T. Wen, "A decentralized design for group alignment and synchronous rotation without inertial frame information," in *Proc. 46th IEEE Conf. Decision Control*, 2007, pp. 2552–2557.

[29] L. Scardovi, A. Sarlette, and R. Sepulchre, "Synchronization and balancing on the N-tours," *Syst. Control Lett.*, vol. 56, no. 5, pp. 335–341, 2007.

[30] L. Scardovi, R. Sepulchre, and N. E. Leonard, "Stabilization laws for collective motion in three dimensions," in *Proc. Eur. Control Conf.*, 2007, pp. 4591–4597.

[31] E. W. Justh and P. S. Krishnaprasad, "Natural frames and interacting particles in three dimensions," in *Proc. 44th IEEE Conf. Decision Control Eur. Control Conf.*, 2005, pp. 2841–2846.

[32] Y. Igarashi, T. Hatanaka, M. Fujita, and M. W. Spong, "Passivity-based 3D attitude coordination: Convergence and connectivity," in *Proc. 46th IEEE Conf. Decision Control*, 2007, pp. 2558–2565.

[33] R. Murray, Z. Li, and S. S. Sastry, *A Mathematical Introduction to Robotic Manipulation*. Boca Raton, FL: CRC Press, 1994.

[34] F. Bullo and A. D. Lewis, *Geometric Control of Mechanical Systems*. New York: Springer, 2004.

[35] M. Fujita, H. Kawai, and M. W. Spong, "Passivity-based dynamic visual feedback control for three dimensional target tracking:Stability and L2-gain performance analysis," *IEEE Trans. Control Syst. Technol.*, vol. 15, no. 1, pp. 40–52, Jan. 2007.

[36] M. W. Spong, S. Hutchinson, and M. Vidyasagar, *Robot Modeling and Control*. New York: Wiley, 2006.

[37] A. Papachristodoulou and A. Jadbabaie, "Synchronization in oscillator networks with heterogeneous delays, switching topologies and nonlinear dynamics," in *Proc. 45th IEEE Conf. Decision Control*, 2006, pp. 4307–4312.

[38] M. Ji and M. Egerstedt, "Distributed coordination control of multiagent systems while preserving connectedness," *IEEE Trans. Robot.*, vol. 23, no. 4, pp. 693–703, Aug. 2007.

[39] M. M. Zavlanos and G. J. Pappas, "Potential fields for maintaining connectivity of mobile networks," *IEEE Trans. Robot.*, vol. 23, no. 4, pp. 812–816, Aug. 2007.

[40] S. Boyd, "Convex optimization of graph Laplacian eigenvalues," in *Proc. Int. Congr. Math.*, 2006, pp. 1311–1319.

[41] Y. Kim and M. Mesbahi, "On maximizing the second smallest eigenvalue of a state-dependent graph Laplacian," *IEEE Trans. Autom. Control*, vol. 51, no. 1, pp. 116–120, Jan. 2006.

[42] M. Carmela, D. Gennaro, and A. Jadbabaie, "Decentralized control of connectivity for multi-agent systems," in *Proc. 45th IEEE Conf. Decision Control*, 2006, pp. 3629–3633.
[43] J. Hespanha, O. A. Yakimenko, I. I. Kaminer, and A. M. Pascoal, "Linear parametrically varying systems with brief instabilities: An application to vision/inertial navigation," *IEEE Trans. Aerosp. Electron. Syst.*, vol. 40, no. 3, pp. 889–900, Mar. 2004.
[44] L. Moreau, "Stability of multiagent systems with time-dependent communication links," *IEEE Trans. Autom. Control*, vol. 50, no. 2, pp. 169–182, Feb. 2005.
[45] Y. Fang, K. A. Loparo, and X. Feng, "Inequalities for the trace of matrix product," *IEEE Trans. Autom. Control*, vol. 39, no. 12, pp. 2489–2490, Dec. 1994.
[46] R. A. Horn and C. R. Johnson, *Matrix analysis*. Cambridge, U.K.: Cambridge University Press, 1985.
[47] H. K. Khalil, *Nonlinear Systems*, 3rd ed. Englewood Cliffs, NJ: Prentice-Hall, 2002.

Yuji Igarashi received the B.E. and M.E. degrees in control and systems engineering from Tokyo Institute of Technology, Tokyo, Japan, in 2006 and 2008, respectively.

He is currently with the Advanced Technology R&D Center, Mitsubishi Electric Corporation, Hyogo, Japan. His research interests include cooperative control.

Takeshi Hatanaka received the B.Eng. degree in informatics and mathematical science, and the M.Inf. and Ph.D. degrees in applied mathematics and physics from Kyoto University, Kyoto, Japan, in 2002, 2004, and 2007, respectively.

He is currently an Assistant Professor with the Department of Mechanical and Control Engineering, Tokyo Institute of Technology, Tokyo, Japan. From 2006 to 2007, he was a research fellow of the Japan Society for the Promotion of Science at Kyoto University. His research interests include cooperative control, mobile sensor networks and predictive control.

Masayuki Fujita received the B.E., M.E., and Dr. of Engineering degrees in electrical engineering from Waseda University, Tokyo, Japan, in 1982, 1984, and 1987, respectively.

Since 2005, he has been a Professor of the Department of Mechanical and Control Engineering, Tokyo Institute of Technology, Tokyo, Japan. From 1985 until 1992, he was with the Department of Electrical and Computer Engineering, Kanazawa University, Kanazawa, Japan. He was on the faculty of Japan Advanced Institute of Science and Technology as an Associate Professor from 1992 to 1998 and Kanazawa University as a Professor in 1999. From 1994 to 1995, he held a visiting position with the Department of Automatic Control Engineering, Technical University of Munich, Munich, Germany. His research interests include robust control and its applications, cooperative control and passivity-based visual feedback.

Dr. Fujita was a recipient of the 2008 IEEE Transactions on Control Systems Technology Outstanding Paper Award, the Best Paper Award from the Society of Instrument and Control Engineers (SICE) in 1997, and from the Institute of Systems, Control and Information Engineers (ISCIE) in 2000. He will serve the General Chair of 2010 IEEE Multi-conference on Systems and Control. He is currently Board of Governor of the IEEE Control Systems Society, an Editor of the *SICE Journal of Control, Measurement, and System Integration* and Associate Editor of *Automatica*. He also served as an Associate Editor of the IEEE TRANSACTIONS ON AUTOMATIC CONTROL and Asian *Journal of Control*.

Mark W. Spong (F'96) received the D.Sc. degree in systems science and mathematics from Washington University, St. Louis, in 1981.

From 1984–2008 he was at the University of Illinois at Urbana-Champaign. Currently, he is Dean of Engineering and Computer Science at the University of Texas at Dallas and holder of the Lars Magnus Ericcson Chair in Electrical Engineering. His research interests include robotics and nonlinear control. He has published more than 250 technical articles in control and robotics and is coauthor of 4 books.

Dr. Spong was a recipient of recent awards including the IEEE Transactions on Control Systems Technology Outstanding Paper Award, the IROS Fumio Harashima Award for Innovative Technologies, the Senior Scientist Research Award from the Alexander von Humboldt Foundation, the Distinguished Member Award from the IEEE Control Systems Society, the John R. Ragazzini and O. Hugo Schuck Awards from the American Automatic Control Council,and the IEEE Third Millennium Medal. He is Past President of the IEEE Control Systems Society and past Editor-in-Chief of the IEEE TRANSACTIONS ON CONTROL SYSTEMS TECHNOLOGY.